VULNERABLE ROAD USER TRANSIT OPTIMIZATION WITH HEALTHCARE PRIVATIZATION (VRUTOP)

FINAL REPORT

August 2023

Hyoshin Park, PhD

North Carolina Agricultural and Technical State University

US DEPARTMENT OF TRANSPORTATION GRANT 69A3551747125

DISCLAIMER

The contents of this report reflect the views of the authors, who are responsible for the facts and the accuracy of the information presented herein. This document is disseminated under the sponsorship of the Department of Transportation, University Transportation Centers Program, in the interest of information exchange. The U.S. Government assumes no liability for the contents or use thereof.

1. Report No.	2. Government Accession No.	3. Recipient's Catalog No.
4. Title and Subtitle Vulnerable Road User Transit Optimization with Healthcare Privatization (VRUTOP)		5. Report Date August 2023 6. Source Organization Code
7. Author(s) Park, Hyoshin, Kai Monast		8. Source Organization Report No. CATM-2023-R4-NCAT
9. Performing Organization Name and Address Center for Advanced Transportation Mobility Transportation Institute 1601 E. Market Street Greensboro, NC 27411		10. Work Unit No. (TRAIS) 11. Contract or Grant No. 69A3551747125
12. Sponsoring Agency Name and Address University Transportation Centers Program (RDT-30) Office of the Secretary of Transportation–Research U.S. Department of Transportation 1200 New Jersey Avenue, SE Washington, DC 20590-0001		13. Type of Report and Period Covered Final Report: February 2019 – February 2023 14. Sponsoring Agency Code USDOT/OST-R/CATM
15. Supplementary Notes:		

16. Abstract. This research focuses on improving the transit service of vulnerable road users while addressing recent trends in Medicaid transformation. One of the most notorious issues is the difficulty of knowing how much added time cushion should be considered for picking-up each user and transit time. This temporal time uncertainty will be uniquely formulated by taking advantage of the data collected before and after the Medicaid transformation, which will make this research a pioneer in demand response transportation systems. From the user's perspective, an adaptive trip planner considers the real-time impact of environment changes on pedestrian route choice preferences and tolerance level in response to transit service uncertainty. Sidewalk inventory is integrated in directed hypergraph on the General Transit Feed Specification to specify traveler utilities as weights on the hyperedge. A realistic assessment of the effect of the user-defined preferences on a traveler's path choice is presented for a section of the Boston transit network, with schedule data from the Massachusetts Bay Transportation Authority. Different maximum utility values are presented as a function of varying travelers' risk-tolerance levels. In response to unprecedented climate change, poverty, and inflation, this new trip planner can be adopted by state agencies to boost their existing public transit demand without extra efforts.

17. Key Words First Mile Trip, Mobility as a service, Medicaid transformation, Dwell time uncertainty, Paratransit, Reinforcement Learning	18. Distribution Statement Unrestricted; Document is available to the public through the National Technical Information Service; Springfield, VT.

19. Security Classif. (of this report) Unclassified	20. Security Classif. (of this page) Unclassified	21. No. of Pages 49	22. Price ...

Form DOT F 1700.7 (8-72) Reproduction of completed page authorized

TABLE OF CONTENTS

EXECUTIVE SUMMARY

Current free and subscription-based trip planners have heavily focused on providing available transit options to improve the first- and last-mile connectivity associated with a destination. However, those trip planners may not truly be multimodal to vulnerable road users (VRUs) since the selected sidewalk routes may not be accessible or feasible for people with certain disabilities. Depending on the level of availability of digital twin of travelers' behaviors and sidewalk inventory, providing a personalized suggestion about the sidewalk with route features coupled with transit service reliability could be useful and happier transit riders may boost public transit demand/funding and reduce rush hour congestion. This research focuses on improving the transit service of vulnerable road users while addressing recent trends in Medicaid transformation. One of the most notorious issues is the difficulty of knowing how much added time cushion should be considered for picking-up each user and transit time. This temporal time uncertainty will be uniquely formulated by taking advantage of the data collected before and after the Medicaid transformation, which will make this research a pioneer in demand response transportation systems. From a user perspective, an adaptive trip planner considers the real-time impact of environment changes on pedestrian route choice preferences and tolerance level in response to transit service uncertainty. Sidewalk inventory is integrated in directed hypergraph on the General Transit Feed Specification to specify traveler utilities as weights on the hyperedge. A realistic assessment of the effect of the user-defined preferences on a traveler's path choice is presented for a section of the Boston transit network, with schedule data from the Massachusetts Bay Transportation Authority. Different maximum utility values are presented as a function of varying travelers' risk-tolerance levels. In response to unprecedented climate change, poverty, and inflation, this new trip planner can be adopted by state agencies to boost their existing public transit demand without extra efforts.

1. INTRODUCTION

Eighty-nine percent of the U.S. population is projected to live in urban areas by 2050 and more than 300 urban areas having populations above 100,000 spark greater demand for multimodal transit. Recent widespread food insecurity and housing instability have magnified the already extreme income inequities and accessibilities. Vulnerable road users (VRUs) walk and bike to reach transit, food, jobs, and medical services while temperatures dive from record highs to freezing. While one in five North Carolinians will be at least 65 years old needing other accessible alternatives to driving, current free and subscription solutions, such as Google Maps and GoTriangle, fail to incorporate detailed access information for people with personal preference and mobility limitations. In response to unprecedented climate change, poverty, and inflation, we need a multimodal trip planner more than ever. Happy transit riders play an important role in boosting public transit demand/funding and reducing rush hour congestion.

North Carolina's GoTriangle planner provides travel options to commuters by referencing Google Transit routes. However, GoTriangle does not provide integrated mobility and accessibility options for NC travelers. The trip planner does not connect transit options to other modal options (e.g., bikes, e-scooter, etc.). Each trip option only provides estimated walking time to/from transit stops without considering the accessibility. The Massachusetts Bay Trip planner is the only successful tool to integrate mobility information about sidewalk slope, surface, width, and shade. It takes great effort and time to develop a trip planner tool that reflects local community needs and deliver multimodal transportation safely and equitably. In this project, unlike other trip planners, Multi-Modal Optimal Dynamic pErsonalized (M2ODE) trip planner recommends the transit options including accessible and feasible sidewalk routes for travelers in the pedestrian modes. This project investigates both the system and user side of the trip planner that have different goals and objectives; therefore, although this project's main focus is on VRUs, Sections 2 and 3 of this report addresses two different problems.

2. TRIP PLANNER MODE (MULTIMODAL OPTIMAL DYNAMIC PERSONALIZED)

Recent work done by authors of this study developed VRU Personalized Optimized Dynamic (VRUPOD) [1] trip planner to provide personalized sidewalk route guidance for users who save personal information relevant to transportation needs (e.g., stamina and ability to traverse uneven terrain) and publicly available information about route nodes, elevation changes, weather, and traffic etc. This project integrates utilities of transit route choices with sidewalk route choices associated with individual needs and capabilities (Figure 1).

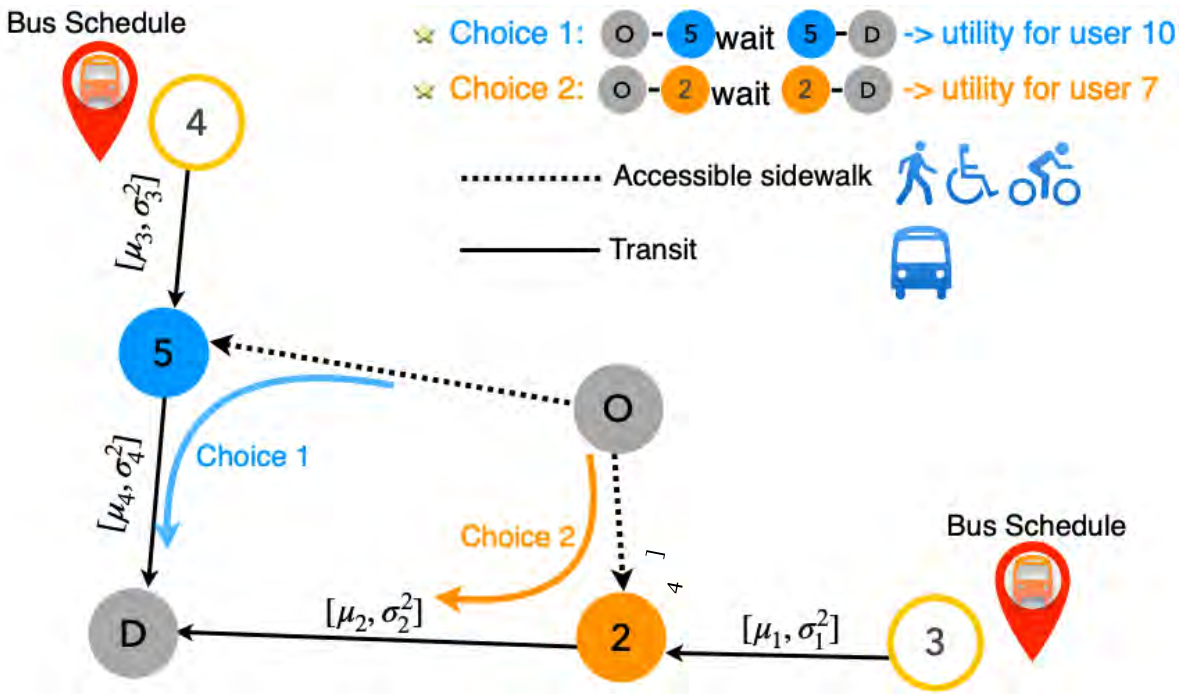

Fig. 1: M^{2}ODE trip planning with best path recommendation: To go from origin **O** to destination **D**, the traveler's multimodal options, including sidewalk (e.g., walk, bike) or transit (e.g., bus), depends on availability and anticipated conditions on these modes.

This project addresses the limitations of existing linear shortest cost algorithms in multimodal trip planning due to dynamic interactions between environmental parameters and user preferences. It introduces an adaptable model that considers various modes of

transportation, changing environmental conditions, and user preferences over time. By incorporating travel time uncertainties and travelers' tolerance levels, the proposed multimodal trip planner provides personalized path recommendations. The model combines pedestrian and transit mode decisions using a heuristic approach and utility maximization. The paper utilizes the hypergraph framework [2], [3], [4], [6] to model the transit schedule network and presents a numerical example to estimate anticipated travel time variability and offers a novel approach for personalized path accessibility considering multimodal transportation and traveler preferences.

2.1. LITERATURE REVIEW

While there is a rich history of trip planners for the transit mode, the pedestrian mode with preferences has received less attention, thus there is an absence of full integration of both pedestrian and transit modes. This is critical since individuals with mobility issues, such as elderly persons or wheelchair users, are more sensitive to uncertainties in services.

2.1.1 TRIP PLANNER FOR PEDESTRIAN MODE

Undoubtedly, navigation systems that integrate user preferences find routes that are more suitable for VRUs than the shortest routes [5], [8], [9]. VRUs encounter a range of obstacles impeding easy navigation in the sidewalk network [10]. Existing designs of public transportation systems do not entirely fulfill the needs of people with disabilities in terms of mobility and accessibility though they are user centered [7], [9], [11]. Though existing design may offer personalized routing, it lacks in multimodality [12]. Identifying and avoiding inaccessible places in the current pavement network as a short-term solution instead of redesigning urban transportation and sidewalk networks as a long-term solution can accelerate helping VRUs [13]. Applications such as the OpenRouteService provides a single American Disability Association (ADA)-compliant path for a baseline level of accessibility. Such "one-size-fits-all" approaches to different pedestrian mobility need only ensure that pedestrians fitting a particular description (e.g., wheelchair user) can use the path specified. However, the

path for many mobility-impaired people requires consideration of their specific needs and capabilities.

This project develops the pedestrian model with the following contributions. First, the pedestrian model accommodates the various sidewalk factors: width, slope, surface type, and length, identified to influence users' path choice significantly [8], [14], [15], to improve the safety and mobility for people with mobility impairments who walk and use transit in urban and suburban environments. Second, the pedestrian model accommodates changing preferences and the interaction effect between sidewalk variables and weather conditions contributing to a path choice.

2.1.2 TRIP PLANNER FOR TRANSIT MODE

The majority of studies on transit accessibility and route choice decisions for flexible/fixed transit have focused on travel time as the only measure for planning route choice, though some have accounted for attributes such as monetary fare [16], [17]. Consequently, minimizing the expected travel time has been widely developed for evaluating transit route choice [18]. For transit trip planning purposes, the most common method of estimating the expected travel time is to use the schedule-based data in a standard format known as the General Transit Feed Specification (GTFS) [19]. OpenTripPlanner utilizes GTFS data and pedestrian networks (e.g., OpenStreetMap) for route planning. However, relying solely on schedules has limitations, such as under/overestimating travel time and disregarding congestion and variability. Traditional route choices prioritize minimizing schedule travel time, neglecting real-time delays and urban peak-hour variations.

The availability of automatic vehicle location (AVL) data allows transit system managers to measure day-to-day travel time variability on transit links. This data can be used to improve traveler's accessibility and route choice decisions by considering anticipated variability. Previous studies have shown the impact of travel time variability on transit route choices [20], [21], but integrating traveler's perception of this variability is lacking. This research contributes to

personalized path accessibility models by incorporating traveler's perception of variability, even if it does not result in the lowest expected schedule travel time.

The widespread collection and availability of AVL data can support characterizing the reliability of transit networks. AVL data can estimate the anticipated travel time variability on transit links for a given period and day before making route choice decisions. Anticipating and integrating the travel time variability as a measure of reliability for planning route choice can provide more rational routes according to the traveler's perception of the anticipated variability, even if such route is not one with the minimum schedule travel time. Even for driving, the inclusion of reliability in route choice and accessibility modeling is still at an exploratory stage [22].

2.1.3 INTEGRATED MULTIMODAL NETWORKS

Studies on integrating first/last mile connections with flexible/fixed transit in multimodal networks are popular in literature [23]. The emphasis has been on integrating modes such as electric scooters, bike-sharing, and car-sharing with fixed transit in a decentralized problem with less attention on pedestrian modes (e.g., sidewalk) [24], [25], [26], [27]. Still, those considering pedestrian modes are limited to recommending the shortest sidewalk path to users in getting to/from transit stops and other destinations in the pedestrian network. In addition, the existing framework for integrating pedestrian connections is based on each mode's local routing [24], [25]. However, there are several concerns on the benefit of the current multimodal framework. First, rather than the shortest path, considering the accessibility of VRUs in the path model will improve the mobility of VRUs. Second, building pedestrian connections to fixed transit in multimodal networks needs to guarantee a smooth transfer between the modes.

Our approach calculates the most accessible sidewalk path for pedestrians based on an ADA [28] standard measure. We narrow down the sidewalk network to a spatial region centered around the traveler's location, using the shortest distance between relevant points. This reduces the search space and avoids impractical solutions. The personalized path recommendation considers schedule travel time, anticipated travel time variability, and pedestrian accessibility in a utility maximization model. We also account for the inconvenience

that travelers may tolerate due to variability in transit travel times and waiting times. This is done by incorporating risk-tolerance to anticipated variability. Our model:

- Incorporates the travelers' personalized preference to sidewalk accessibility to/from transit stops and to other destinations
- Accommodates the interaction between sidewalk factors and weather conditions for each sidewalk segment contributing to a path choice.

In addition to expected schedule travel time, the travelers' perception of reliability of the schedule is incorporated as the risk-tolerance on the anticipated travel time variability, modeled as a function of the mean and variance of link/route travel time [29].

2.2. METHODOLOGY

The travelers' preferences for the transit and pedestrian mode decisions are evaluated and combined in a heuristic for the personalized path search. We describe the transit network through nodes representing the origin stop, destination stop, and transit stops along a route, and edges representing the travel time conditions of the road between the nodes (Figure 2) run r is aggregated over several observation periods or days N and used to estimate link and route level travel time variability. Different times of the day are associated with different degrees of variability in link travel time.

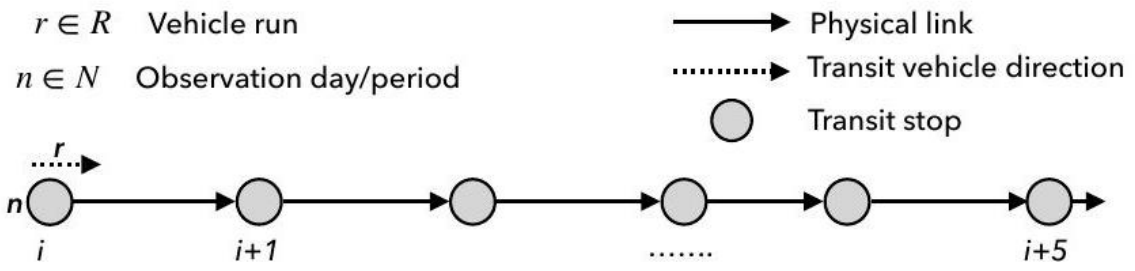

Fig. 2: A transit route with multiple stops showing how the experienced travel time for vehicle

2.1.4 TRANSIT NETWORK DESCRIPTION

This study characterizes the anticipated day-to-day travel time variability for a vehicle run on each link/route in the transit network using historical time at each location from archived AVL data, also known as retrospective GTFS data. Vehicle run refers to the daily assignments for an individual bus. $i \in I$ is the set of transit stops along the route and the set of vehicle runs $r \in R$ allocated to the route. AAT_i^r is the actual arrival time of vehicle run $r \in R$ at stop $i \in I$. The invehicle travel time (IVTT) and the number of days/periods N is given by:

$$IVTT_{i,i+1}^r = AAT_{i+1}^r - AAT_i^r.$$

The anticipated mean (μ) and variance (σ^2) for $IVTT$ is estimated as:

$$\mu_{(i,i+1)}^{(r)} = \frac{\sum_{n=1}^{N} IVTT_{(i,i+1),n}^r}{N}$$

For cases of a normally distributed IVTT for link l, $v(\mu_l, \sigma_l^2)$, this study assumes link travel time variability can be treated as normally distributed random variables. Therefore, the total anticipated $IVTT$ of path $\mathcal{P}$ is defined as the sum of each links anticipated mean and variances of travel time as $\mu_{\mathcal{P}=\sum \mathcal{P}_\mu}$ and $\sigma_{\mathcal{P}=\sum \mathcal{P}\sigma}$. In selecting a transit route, our goal is to evaluate and incorporate the anticipated mean and variance of travel time for feasible alternative routes that satisfy a traveler's PAT at the destination.

1) Transit schedule network: A route service graph for the transit network is expanded to a node-based time graph to capture the temporal information provided through the schedule data (Figure 3). The links connect these nodes to indicate the vehicle run trajectory between consecutive stops. In-vehicle travel time and walking time links are used to indicate movement from one node/stop to another node/stop. The anticipated in-vehicle travel time variability for each link/route is represented through the mean and variance of travel time for the link/route. Given the traveler's origin-destination pair $(O - D)$, a PAT, the first of our twophase solution search procedure, utilizes the node-based time expanded graph in the personalized path accessibility framework.

2) Weighting functions on hyperedge: The directed hypergraph on the transit schedule network associates each hyperedge ω with a real weight vector $\mathbf{w}(\omega)$. Without loss of generality, the component of the weight vector is expected schedule travel time (including walking and waiting time) on the hyperedge. For each feasible path Π that satisfies the travelers PAT at the destination, the weighting function defines a node function $\mathbf{W}_\Pi$ which assigns weights to all its nodes (time expanded stops) depending on the weights of its hyperedges. Given the destination D, $\mathbf{W}_\Pi(D)$ is the weight of the path Π under the chosen weighting function. In this study, we define an additive weight function on each time expanded stop S^n as a function of both the weights of the hyperedges entering into S^n and that of the nodes in their tail (for simplicity, let $y = S^n$):

$$\mathbf{W}_\Pi(y) = \min\{\mathbf{w}(\omega) + \mathrm{F}_\Pi(\mathrm{T}(\omega)) : \omega \in \mathrm{E}_\Pi \cap \mathrm{BS(y)}\},$$
$$y \in V_\Pi \setminus \{s\},$$

where $\mathrm{F}_\Pi(\mathrm{T}(\omega))$ is a function of the weights of the nodes in $\mathrm{T}(\omega)$, and $\mathrm{BS(y)} = \{\omega \in \mathrm{E}: \mathrm{y} \in \mathrm{H}(\omega)\}$ is the backward star of node y representing the incoming edge at node y. F is a nondecreasing function of $\mathbf{W}_\Pi(x)$ for each $x \in T(\omega)$

$$\mathrm{F}_\Pi(\mathrm{T}(\omega)) = \mathrm{F}(\{\mathrm{W}_\Pi(\mathrm{x}) : \mathrm{x} \in \mathrm{T(y)}\}), \omega \in \mathrm{E}_\Pi.$$

3) Cost of anticipated travel time variability: We integrate the travelers' risk-tolerance level concerning the anticipated variability for the best route recommendation, even if such a route is not with the lowest expected schedule travel time. We propose the exponential utility function $u(\Pi) = -(\mathrm{sgn}\,(\lambda))e^{-\lambda\Pi}$, to characterize the traveler's preference to the anticipated travel time variability for transit links on feasible path Π. The local measure of risk-tolerance, known as the Arrow-pratt measure of absolute risk-aversion at Π, is $\frac{-u''(\Pi)}{u'(\Pi)} = \lambda$. The representations $u'(\Pi)$ and $u''(\Pi)$ are the first and second derivative of $u(\Pi)$. The values of $\lambda \neq 0$ represents the risk-tolerance coefficient with the sign of λ (sgn). The mean-variance approximation is the sum of the anticipated mean travel time (μ) and the risk $\left(\frac{\sigma^2}{2}\right)$ multiplied by the risk-tolerance coefficient (λ), representing $M_\Pi = \mu_\Pi + \frac{\lambda\sigma_\Pi^2}{2}$

as the balance between mean and variance of IVTT on feasible path Π. The generalized cost function in the transit route choice is defined to find the strategy that minimizes the sum of traveler's cost on (1) expected schedule travel time and (2) the anticipated travel time variability adjusted for the traveler's risk tolerance.

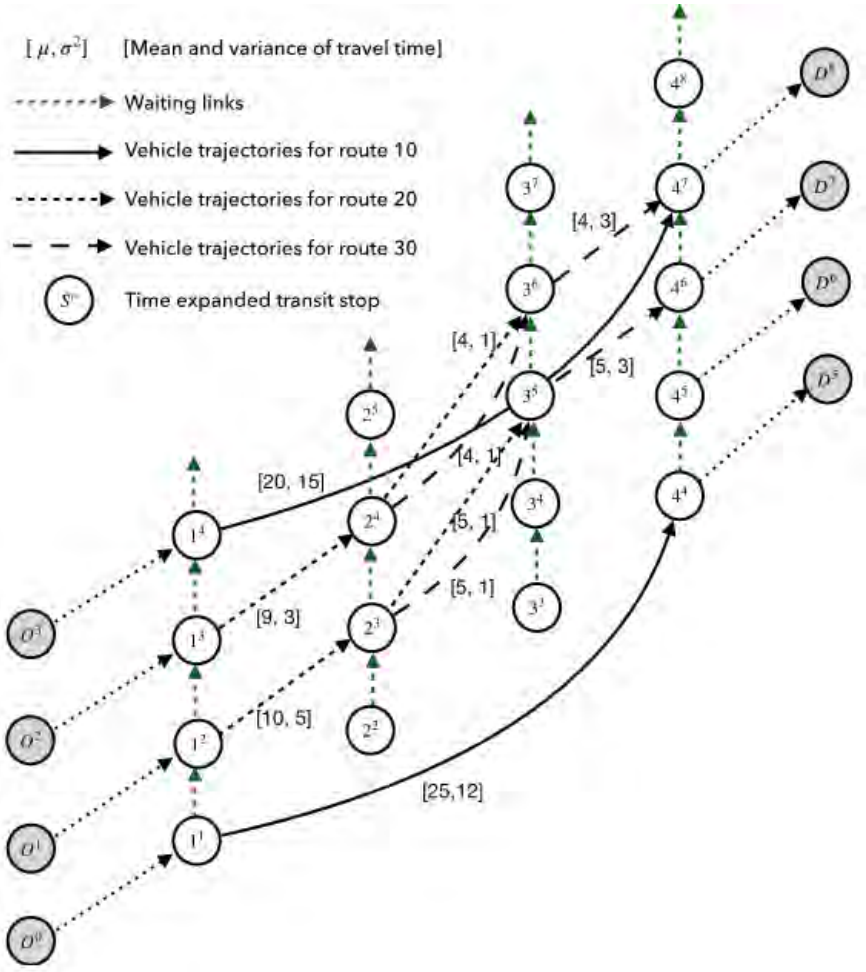

Fig. 3: A Node-based representation of a transit network showing the time expanded transit stops. The nodes have space-time coordinates representing the different times of transit vehicle availability according to the schedule. Specifically, every stop is (a) expanded based on points in time when a vehicle from a route will visit, and (b) the time points are connected and expanded spatially by each vehicle run (or route).

2.1.5 SIDEWALK ACCESSIBILITY MEASURE

Relating to previously established research [30], [31], we develop five parameters: width, length, slope, sidewalk surface type, and weather condition to characterize the accessibility of each sidewalk segment. The sidewalk network is represented as a graph $\mathcal{G} = (\mathcal{N}, \mathcal{E})$, where $n \in \mathcal{N}$ is the set of nodes and $e \in \mathcal{E}$ is the set of edges. By assuming a spatial region (Radius ($\mathcal{R}$) equal to the shortest distance between two locations) we reduce the search space and also prevent finding infeasible solutions due to long distances. A traveler can move from node n to node n' if an edge connects the two nodes. The cost of each edge is based on parameters that define sidewalk accessibility for that edge for the traveler [1]. The interaction effect between sidewalk variables can limit the accessibility of sidewalk segments.

This project considers five surface types based on field survey: concrete (best), asphalt, brick, cobblestone, and gravel (worst). Three levels of weather conditions are considered:sunny (best), rainy, snowy (worst)[1]. With appropriate adjustments to Eq. (4), the sidewalk path considering the travelers sidewalk accessibility preferences is found. Specifically, if we consider the arrival time at a destination n_d (e.g., final destination D satisfying the PAT), the optimal sidewalk path minimizes the total cost for a given origin-destination pair (n_o, n_d) :

$$\mathbf{S}_{\Pi}(n) = \min\{\mathbf{s}(e) + \mathrm{S}_{\Pi}(\mathrm{T(e)}) : \mathrm{e} \in \mathcal{E} \cap \mathrm{BS(n)}\},$$
$$n \in \mathcal{N}\{\}.$$

2.3. EVALUATION

2.3.1. ESTIMATION OF IN-VEHICLE TRAVEL TIME VARIABILITY

Using retrospective GTFS data, a temporal aggregation of link-level travel time is used to estimate the anticipated IVTT variability. Retrospective GTFS data capture significant travel time variations for each vehicle run, providing a more realistic representation of the anticipated travel time variability. A statistical measure of each link-level variability defined by the mean and standard deviation of travel time is constructed for each day in the weekday as shown in Figure 4.

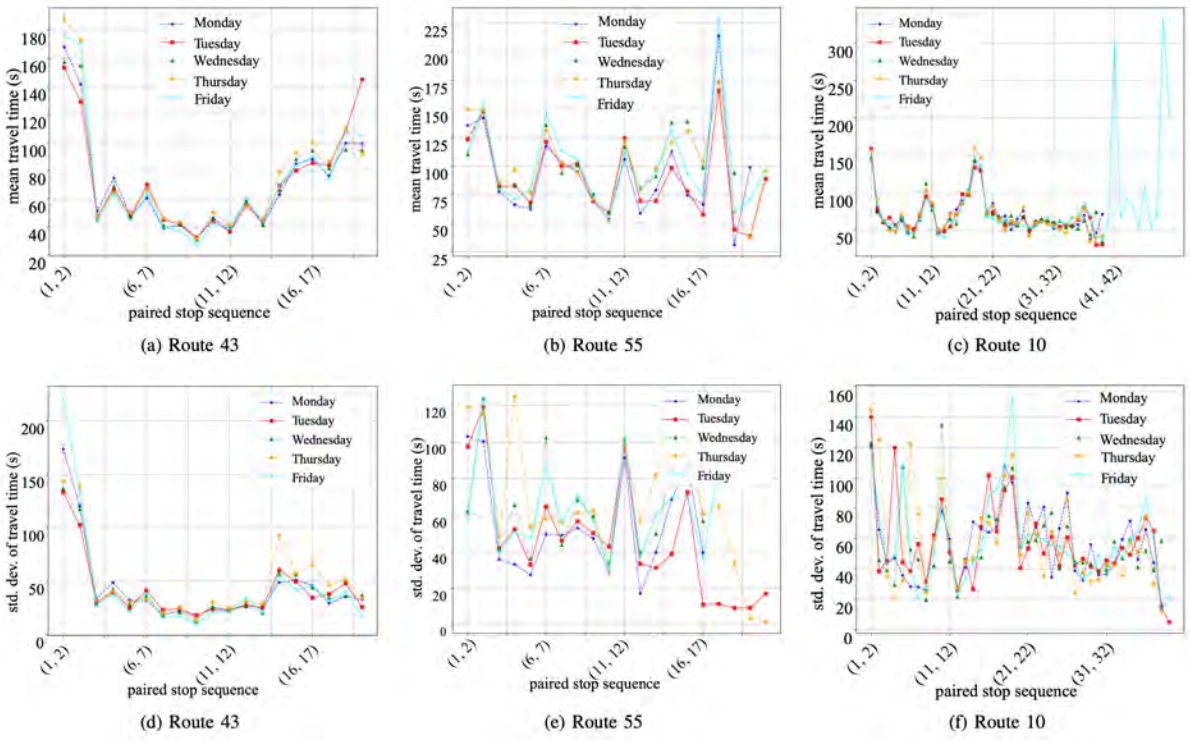

Fig. 4: Estimated day-to-day IVTT variability for routes 43, 55, and 10 for the period between 5:00 and 8:00 am from historical AVL data. The estimates show significant travel time variability for most links. Specifically, we see that several links on routes 43, 55, and 10 have high values of anticipated standard deviations for the period between 5:00 and 8:00 a.m. For example, looking at the link (1,2) on route 43 (Figure 4a and Figure 4d), the variability profile shows a significantly high standard deviation ($\approx$ 220 s) compared to the mean travel

time ($\approx$ 170 s) for Friday. This implies high volatility concerning the anticipated travel time on the link. The link-level travel time variability is easily extended to multiple consecutive links/routes as described in Section III-A.

2.3.2. IMPACT OF RISK-TOLERANCE ON TRAVELERS ROUTE SELECTION

Considering the anticipated travel time variability for the links/routes, the mean-variance approximation with travelers' risk-tolerance evaluates the inconvenience travelers are willing to experience due to these variability. Figure 5 shows the impact of the anticipated travel time variability on the route choice given the traveler's risk-tolerance coefficient.

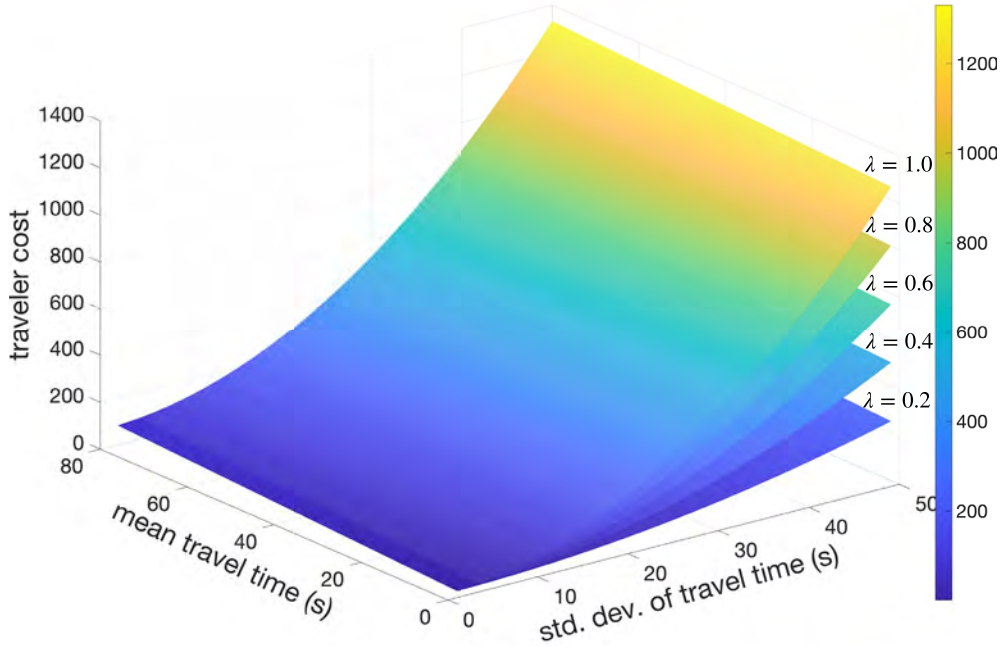

Fig. 5: Variation of travelers' cost for different risk-tolerance. The traveler's cost decreases with decreasing uncertainty (i.e., standard deviation) in travel time, indicating that the traveler will prefer a route with less volatility. We also see that the higher the risk-tolerance coefficient, the higher the traveler's sensitivity to anticipated travel time variability. Therefore, travelers with high risk-tolerance coefficient are less likely to select options with high standard deviations. For example, for the same variability profile (e.g., $\mu = 2, \sigma = 50$), the traveler with a risk-tolerance coefficient of 0.2 has a lower travel cost (≈ 250) than the

traveler with a risktolerance coefficient of 0.4 (cost ≈ 500). This implies that the traveler ($\lambda = 0.4$) perceives this route option as too costly compared to the other traveler ($\lambda = 0.2$)

The indifference curves shown in Figure 6 provide a 2-D contour representation of the travelers' perceived cost to the anticipated travel time variability.

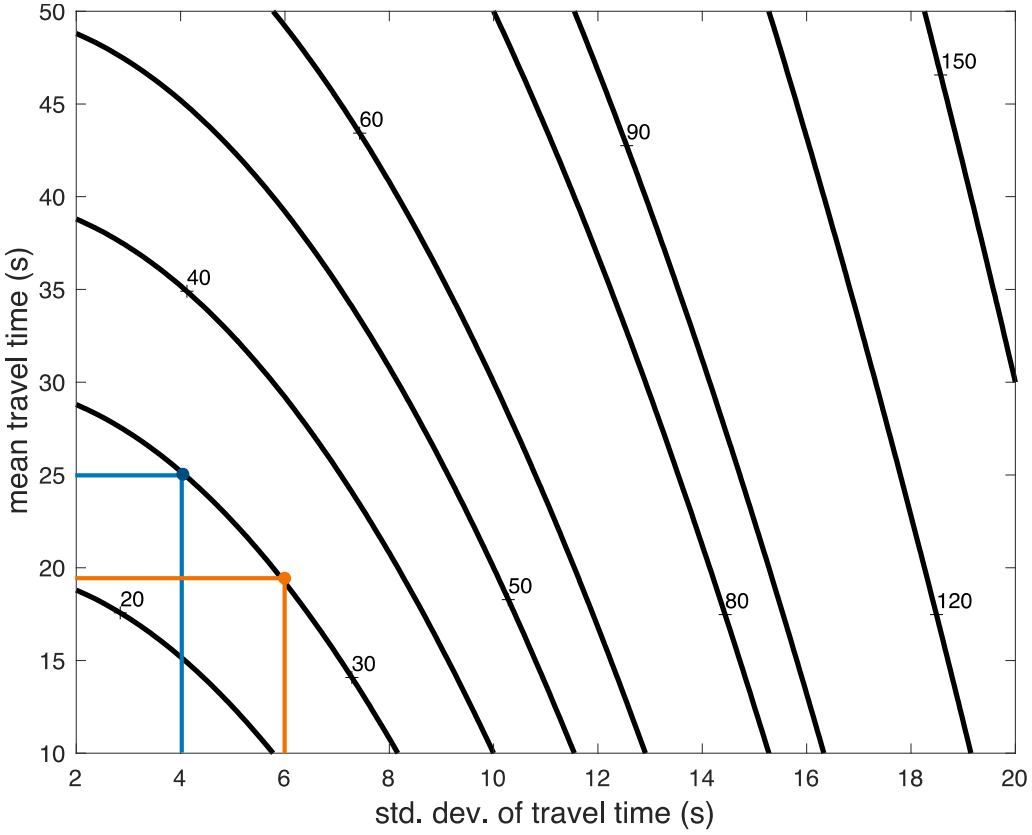

Fig. 6: Indifference curves considering risk-tolerance coefficient ($\lambda = 0.6$). Points on the curves represent different mean and standard deviation combinations of travel time. For routes whose variability profiles result in the same cost, the traveler is indifferent to choosing among the routes. Such alternatives present the same level of inconvenience willing to be experienced by the traveler. For example, looking at the points (representing link/route options) with variability profiles $\mu = 25, \sigma = 4$ and $\mu = 19, \sigma = 6$, the traveler will be indifferent to selecting among these options since both result in the same cost.

2.3.3. ACCESSIBLE SIDEWALK PATH COMPARED TO SHORTEST PATH

To evaluate the proposed pedestrian accessibility model independently, we conduct two experiments for different origin destination pairs in an 8×8 sidewalk grid network (data from Boston sidewalk inventory) and then compute the total score for sidewalk surface type and slope.

The preferences of two users utilized in the experiment is summarized as: User1: High rating for surface type compared to slope, width, and distance (the lower the sidewalk surface type score, the better the sidewalk path), and User2: High rating for slope compared to width, surface type, and distance (the lower the sidewalk slope score, the better the sidewalk path).

Figure 7 shows the comparison bar graphs for surface type and slope scenarios. While we have presented an elementary evaluation, the pedestrian accessibility model is adaptable to a wide range of sidewalk and weather conditions [1].

2.3.4. RESULTS OF PATH RECOMMENDATIONS CONSIDERING DEGREE OF RISK-TOLERANCE

The simulation-based evaluation for a typical day of the week (i.e., Tuesday) shows the best path recommendation with the normalized cost of each feasible path alternative, and the weights β on the cost $(\beta_1 = -2, \beta_2 = -1, \beta_3 = -2)$. In effect, our simulation assumes the expected schedule travel time and the cost of the pedestrian accessibility model are twice as important as the cost of anticipated travel time variability. As described above, the following components are considered for each feasible path; (1) sidewalk cost estimated from the pedestrian accessibility model, (2) transit cost estimated from the mean-variance function due to anticipated traveltime variability, and (3) total expected schedule travel time (including waiting and walking time). The users preference concerning the sidewalk factors is set as: High rating for slope compared to width, length, and surface type.

Figure 8 shows the results for trips from all stops (origins) to one designated destination (All-to-one). We assume a destination stop 10, PAT $= 6{:}30\text{a} \cdot \text{m}$, and PAT time window $dt = 15$ min. Each route has a total of 4 trips that contribute to sub-paths satisfying the PAT with two transfer points (4 and 6). Walking from locations 7 to 6 is based on the optimal sidewalk path. The waiting time at a stop in each feasible path is calculated as the difference between schedule departure time and the expected arrival time.

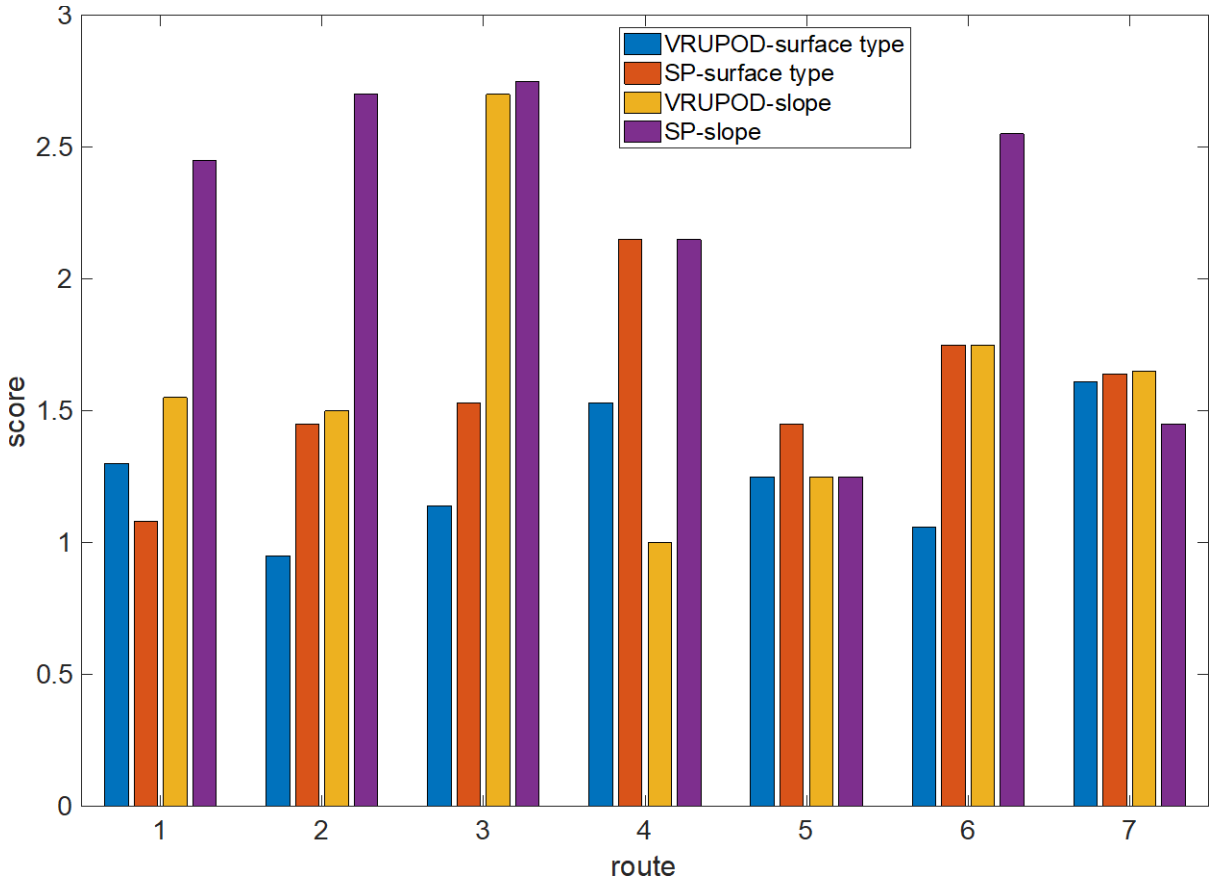

Fig. 7: Surface type and slope score comparison between VRUPOD and Shortest Path (SP).

85.71 percent of sidewalk paths recommended by the VRUPOD method have the lowest average sidewalk surface type score. In the second test, as shown in Figure 7, 71.42 percent of sidewalk paths recommended by VRUPOD have the lowest average sidewalk slope score. This implies that VRUPOD path suggestions are affected by the users' preferences. This

interaction effect allows VRUPOD to select the appropriate sidewalk segments for the optimal path.

In special cases, the static waiting time estimation can be extended to a more generalized waiting time as a function of bus punctuality. For example, when vehicles are instructed to wait at stops when vehicle arrival time is less than scheduled departure time, we can assume that the normal distributed IVTT between two consecutive stops will mostly lead to a log-normal distributed waiting time at the successive stops. In other words, the distribution for departure time delay for the vehicle runs at the stops is potentially right-skewed. The anticipated travel time variability defined by the mean and variance for *IVTT* for each physical path in a feasible path are computed from the results of the retrospective GTFS data, equal to the sum of mean and variances of travel time of links forming the path.

As seen in Figure 8, the best path (vehicle run) at each stop considering the traveler's risktolerance coefficient of 0.2 is the path with the maximum utility. For example, traveling from origin location one to destination ten has a recommended departure time of 6: 12 a.m using vehicle run 5502, same as location five to ten. However, due to the optimal sidewalk path required to get to stop four to board bus 5502, the recommended departure time is 6:07 a.m.

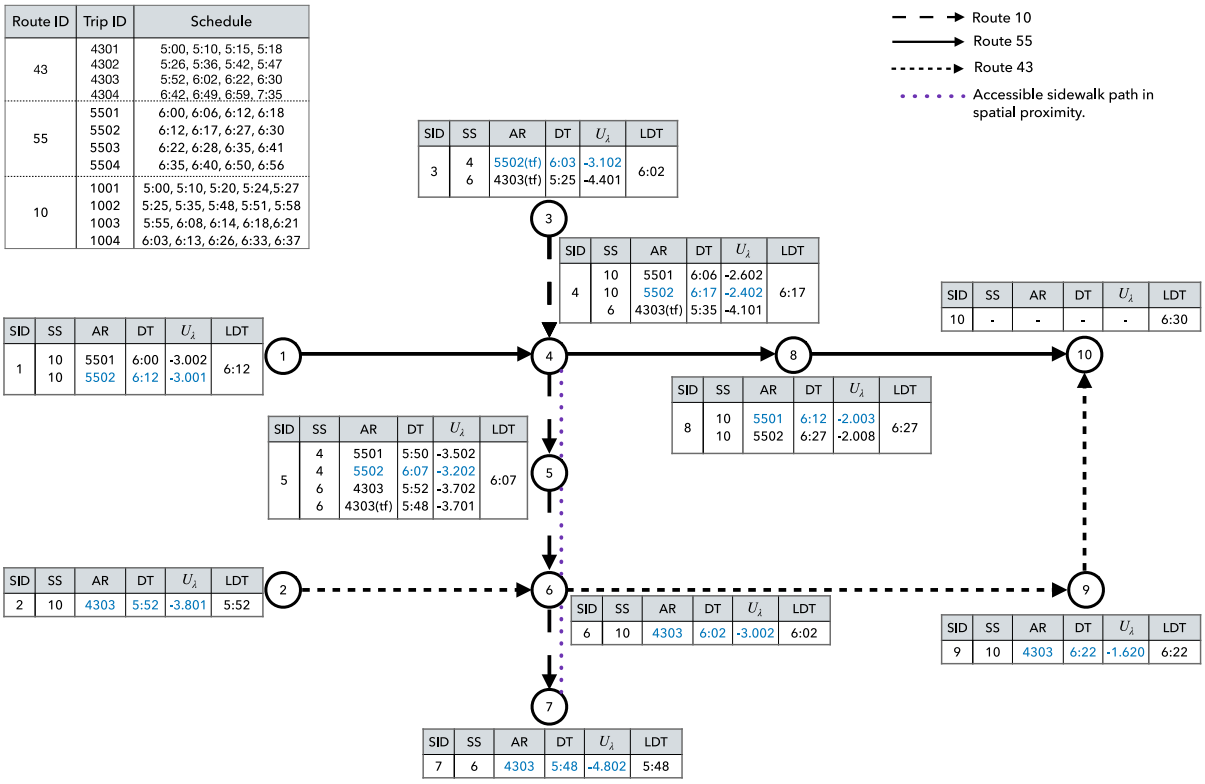

Fig. 8: Modified physical representation of route 10, 43 and 55 from MBTA showing common points. The results of path with utility U_λ for selecting minimum risk path based on the traveler's risk-tolerance at any given stop. SID: Stop ID, SS: Successor Stop, AR: Attractive Run, DT: Departure Time, LDT: Latest Departure Time to ensure arrival within PAT, tf :Transfer. Blue text in the figure shows run (strategy) that will be recommended for a traveler with risk-tolerance coefficient $\lambda = 0.2$.

For example, looking at the path option from location eight to ten and risk-tolerance coefficients 0.2 and 0.4 , we see that the estimated utility for the two path options are simply scaled and so the path recommendation remain the same.

Finally, we compare the path suggestions using the proposed utility function and the trip planner from MBTA for a typical Tuesday (Figure 9).

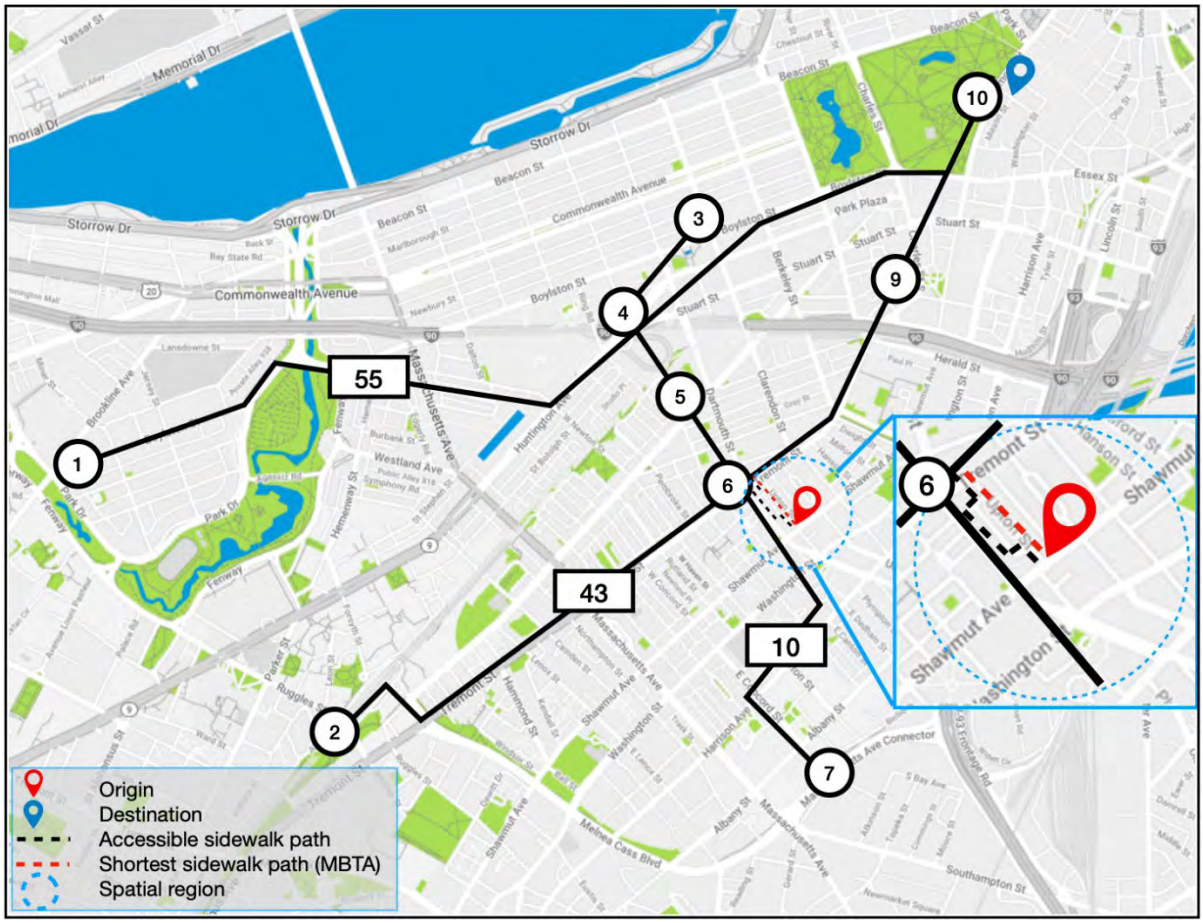

Fig. 9: Paths are evaluated for risk-tolerance coefficients $\lambda = 0.2$ and 1.0 , with pedestrian mode preferences favoring slope and surface type. Using the MBTA trip planner (PAT: 6:30 a.m), suggested departure time is 6:08 a.m. Optimal path includes a 0.3mi sidewalk route to stop 6 , boarding route 43 outbound to final stop ten. Estimated utilities: $\lambda = 0.2$ (-3.010) and $1.0(-3.033)$.

No definite conclusion can be made about the benefits of using our developed framework over the existing trip planners (e.g., MBTA), mainly because the MBTA trip planner option had a lower estimated schedule travel time of 14 min compared to our models' estimated schedule travel time of 20 min. However, we acknowledge that integrating the personalized sidewalk path option that considers the travelers' PAT at the final destination will serve vulnerable road users who are mostly limited in their social activities due to mobility

concerns. In addition, integrating the inconvenience, the travelers are willing to experience will provide a more rational route/path to a traveler's tolerance to ontransit variability.

2.4. CONCLUSIONS

This study develops a multimodal trip planner for VRUs on the pedestrian mode and on-transit travel time, which has been neglected in commercial trip planners. The anticipated variability profile of the links and routes is computed from retrospective GTFS data. The exponential utility approximated by a function of mean-variance of travel time is used to evaluate travelers' risk-tolerance choice to the anticipated in-vehicle travel time variability. A case study is carried out on a simulated test network constructed on a section of the Boston transit network. Depending on the travelers' preferences, including their risk-tolerance to anticipated travel time variability, we find the best path recommendation through a utility maximization approach.

2.5. REFERENCES

[1] J. Darko et al., "Adaptive personalized routing for vulnerable road users," IET Intelligent Transport Systems, vol. 16, no. 3, pp. 10111025,2022.

[2] S. Nguyen et al., "Implicit enumeration of hyperpaths in a logit model for transit networks," Transportation Science, vol. 32, no. 1, pp. 54-64, 1998.

[3] H. Noh et al., "Hyperpaths in network based on transit schedules," Transportation Research Record, vol. 2284, no. 1, pp. 29-39, 2012.

[4] Verbas et al., "Dynamic assignment-simulation methodology for multimodal urban transit networks," Transportation Research Record, vol. 2498, no. 1, pp. 64-74, 2015.

[5] R. E. Alfaris and M. Jalayer, "Assessment of the First-and-Last-Mile Problem in Underserved Communities: Case Study in Camden City, NJ," International Journal of Environmental Research and Public Health, vol. 20, no. 4, p. 3027, 2023.

[6] S. Opasanon and E. Miller-Hooks, "Least expected time hyperpaths in stochastic, time-varying multimodal networks,' Transportation Research Record, vol. 1771, no. 1, pp. 89-96, 2001.

[7] T. Litman, "Evaluating Accessibility for Transport Planning: Measuring Peoples Ability to Reach Desired Services and Activities," March 31,2023.

[8] P. Kasemsuppakorn et al., "Understanding route choices for wheelchair navigation," Disability and Rehabilitation: Assistive Technology, vol. 10, no. 3, pp. 198-210, 2015.

[9] J. M. Owens and A. Miller, "Vulnerable Road User Mobility Assistance Platform (VRU-MAP)," December 2022.

[10] D. Ding et al., "Design considerations for a personalized wheelchair navigation system," in 2007 29th Annual International Conference of the IEEE Engineering in Medicine and Biology Society, IEEE, 2007, pp. 4790-4793.

[11] T. Poldma et al., "Understanding people's needs in a commercial public space: About accessibility and lived experience in social settings," ALTER-European Journal of Disability Research/Revue Europenne de Recherche sur le Handicap, vol. 8, no. 3, pp. 206-216, 2014.

[12] D. Abrantes et al., "A New Perspective on Supporting Vulnerable Road Users Safety, Security and Comfort through Personalized Route Planning," International Journal of Environmental Research and Public Health, vol. 20, no. 4, pp. 3027, 2023.

[13] L. Ferrari et al., "Improving the accessibility of urban transportation networks for people with disabilities," Transportation Research Part Emerging Technologies, vol. 45, pp. 27-40, 2014.

[14] B. Wheeler et al., "Personalized accessible wayfinding for people with disabilities through standards and open geospatial platforms in smart cities," Open Geospatial Data, Software and Standards, vol. 5, no. 1, pp. 1-15, 2020.

[15] A. Gharebaghi et al., "User-specific route planning for people with motor disabilities: A fuzzy approach," ISPRS International Journal of Geo-Information, vol. 10, no. 2, p. 65, 2021.

[16] S. Farber and L. Fu, "Dynamic public transit accessibility using travel time cubes: Comparing the effects of infrastructure (dis)investments over time," Computers, Environment and Urban Systems, vol. 62, pp. 30-40, 2017.

[17] A. El-Geneidy et al., "The cost of equity: Assessing transit accessibility and social disparity using total travel cost," Transportation Research Part A: Policy and Practice, vol. 91, pp. 302-316, 2016.

[18] H. Spiess and M. Florian, "Optimal strategies: A new assignment model for transit networks," Transportation Research Part B: Methodological, vol. 23, pp. 83-102, 1989.

[19] Q. Zervaas, 'Transit Feeds," 2018, accessed 06 March 2021.

[20] W. B. Jackson and J. V. Jucker, "An empirical study of travel time variability and travel choice behavior," Transportation Science, vol. 16, no. 4, pp. 460-475, 1982.

[21] W. Y. Szeto and Y. Wu, "A simultaneous bus route design and frequency setting problem for Tin Shui Wai, Hong Kong," European Journal of Operational Research, vol. 209, no. 2, pp. 141-155, 2011.

[22] Y. Jiang and W. Szeto, "Reliability-based stochastic transit assignment: Formulations and capacity paradox," Transportation Research Part B: Methodological, vol. 93, pp. 181-206, 2016.

[23] Q. Luo, S. Li, and R. C. Hampshire, "Optimal design of intermodal mobility networks under uncertainty: Connecting micromobility with mobility-on-demand transit," EURO Journal on Transportation and Logistics, vol. 10, p. 100045, 2021.

[24] M. Friedrich and K. Noekel, "Modeling intermodal networks with public transport and vehicle sharing systems," EURO Journal on Transportation and Logistics, vol. 6, no. 3, pp. 271-288, 2017.

[25] G. Tang et al., "Bikeshare pool sizing for bike-and-ride multimodal transit," IEEE Transactions on Intelligent Transportation Systems, vol. 19, no. 7, pp. 2279-2289, 2018.

[26] M. Stiglic et al., "Enhancing urban mobility: Integrating ride-sharing and public transit," Computers & Operations Research, vol. 90, pp. 12-21, 2018.

[27] Q. Luo et al., "Multimodal connections between dockless bikesharing and ride-hailing: An empirical study in New York City," in 2018 21st International Conference on Intelligent Transportation Systems (ITSC), IEEE, 2018, pp. 2256-2261.

[28] H. H. Perritt, Americans with Disabilities Act Handbook. Wolters Kluwer, 2002.

[29] R. A. Howard and J. E. Matheson, "Risk-Sensitive Markov Decision Processes," Management Science, vol. 18, pp. 356-369, 1972.

[30] M. Hashemi and H. A. Karimi, "Collaborative personalized multicriteria wayfinding for wheelchair users in outdoors," Transactions in GIS, vol. 21, no. 4, pp. 782-795, 2017.

[31] H. A. Karimi, D. Roongpiboonsopit, and P. Kasemsuppakorn, "Uncertainty in personal navigation services," The Journal of Navigation, vol. 64, no. 2, pp. 341-356, 2011.

3. PROACTIVE PARATRANSIT ROUTING WITH DWELL TIME PREDICTION

A slowly growing national trend on the transition of Medicaid healthcare delivery from predominantly fee-for-service to Managed Care Organization (MCOs) has been recently substantially in- creased. For example, Uber is already transporting passengers for medical appointments in the private sector through its platform, Uber Health. Although contracting with various types of MCOs is expected to reduce Medicaid program costs and better manage utilization of health services, we should also consider disadvantages to other non-Medicaid recipients particularly vulnerable to a decrease in access to other essential destinations. Analyzing the impact of the MCO model in a larger community, particularly on a trade-off between Medicaid recipients and non-recipients re- quires a significant data collection effort. Due to this limitation, existing transit service tools have had difficulties in capturing essential parameters in adjusting to the new environments. Without knowing what specific trends of privatizing Medicaid on where, when, how, have changed the patterns of users of the transit system, it's difficult to improve the efficiency of the service.

Fortunately, the recent remarkable transition toward broker-based privatization of Medi- caid funded service in North Carolina has produced an urgency to analyze the data. While State Agencies are focusing more on investigating system-level changes before and after the Medicaid Transformation, we need to know what specific local community attributes and how combined interaction impacts influence various performance measures of the transit system.

Once a transit is assigned to a set of specific service requests in a sequence, a scheduling software requires to define the pick-up time for each user, which should neither be too long to harm the efficiency nor too short for the user to miss the transit. A wrong estimation of pick-up dwell time could significantly disrupt the schedule due to the discrepancy with the actual schedule. One unit of delay for one user can result in cascading delays for other riders on that vehicles' daily route. As some paratransit riders have serious illnesses, being late for a critical medical appointment can have life threatening implications. Transit systems need to find a way to balance customer ride time with total vehicle time-convenience and efficiency.

Previous studies have addressed the transit scheduling and routing problem with

multiple solution techniques focusing on the online, dynamic, rolling horizon, and stochastic perspectives, while imposing maximum available constraints on the time windows. The study of formulating the temporal uncertainty of time windows into scheduling has been, however, less prevalent in the literature. This research seeks to fill this gap by studying time window uncertainty caused by Medicaid transformation across a collection of pickup and delivery problems with time windows. This research addresses small cities and rural areas (not limited) with little congestion but frequent difficulty in finding the exact pick-up location due to a lack of technology and country roads. Even though there are many urban traffic congestion oriented dynamic rerouting paratransit scheduling and routing algorithms previously developed, the research will be the first explicitly modeling the pick-up and transit time under the impact of Medicaid shifts and improving the efficiency of the transit service.

New scheduling principles are developed to efficiently provide the service. Based on localized attributes, rather than a generalized for all service model, we can optimize the transit service while easily adjusting key parameters based on identified key contributing attributes. Medicaid transformation is a new trend that would change access to health care, which will put the proposed research to be at the frontiers of demand response transportation systems by capitalizing on the main source of unique patterns of Medicaid transformation influencing the service quality.

3.1. LITERATURE REVIEW

The Vehicle Routing Problem (VRP) has received considerable research interest since its intro- duction (*1, 2*). It involves the task of finding optimal routes for a fleet of vehicles to efficiently serve a set of customers or locations. Subsequently, numerous variations of the problem such as PDPTW have been investigated, and alternative solution methods have been suggested (*3–6*). For more comprehensive review, recent surveys of the VRP literature are available (*7, 8*).

There are two operation schemes available: offline and online. In the offline setting, pas- sengers are required to reserve a ride in advance, allowing sufficient time for vehicle routes to be planned by matching requests. Information about daily operations is shared with

both passengers and drivers. On the other hand, the online setting enables real-time interaction among stakeholders. Passengers can request service whenever they need it, and operators can assign them to vehicles almost immediately. This makes the online setting more responsive to unexpected events such as last-minute cancellations or vehicle breakdowns.

In this study, we focus on the paratransit services and aim to enhance the models for dwell time (service time) at customer nodes. Dwell time has a significant impact on the on-time per- formance of paratransit services and other transportation modes (*9–12*). Contrary to common perception, dwell time accounts for a substantial portion of overall trip time, ranging from 26% to 50% (*13*). However, accurately predicting dwell time remains a significant challenge due to several uncontrollable factors such as traveler behavior, mobility needs, among others.

Certain recurrent disturbances can be relatively easier to predict. For instance, loading/ unloading delays can be anticipated if a rider arrives late at a meeting point or requires assistance devices like a wheelchair. Moreover, it is reasonable to suspect that a significant relationship exists between the spatiotemporal characteristics of a location and the potential delay it may cause. While traffic conditions can contribute to uncertainty, they can be mitigated by vehicle detours and avoiding congested areas. However, passengers cannot be left behind. Hence, this study suggests incorporating dwell time uncertainty into paratransit operation systems.

Previous research has proposed various methods for estimating dwell time. Some studies have observed the actual dwell time and used statistical measures such as mean or distributions, while others have employed constant values for system-wide application (*14, 15*). Majority of stud- ies have focused on applying different linear regression models (e.g., multiple, log-linear, quantile, etc.), considering attributes such as the type of vehicle used, and passenger characteristics (*16–20*). However, these models have been found to exhibit poor accuracy in estimating dwell time, often leading to significant underestimation or overestimation, due to their reliance on certain assump- tions. Specifically, linear regression models assume that the variance of the data remains constant across all values of the

dependent variable. This assumption are often not true for dwell time mod- els, as the variance of the data varies depending on the value of the dependent variable. Multiple linear regression have been proposed for analysis to adjust dwell time for paratransit services (21). This approach offers a comprehensive analysis of various independent variables. However, it over- looks potential interactions between variables and assumes linearity in the relationships. Similar studies have focused on incorporating variable or deterministic dwell time for scheduling transit system (22–24). However, these approaches have inherent limitations when it comes to accurately capturing the uncertainties of dwell time during the scheduling process.

In order to enhance the efficiency and reliability of paratransit and bus transportation systems, it is essential to consider the implementation of a dynamic dwell time mechanism that can adapt in real-time as customer requests are fulfilled. Such a mechanism holds great potential for effectively addressing uncertainties inherent in operational conditions and significantly improving the accuracy of routing and scheduling decisions. By continuously updating dwell time estimates based on the progress of service delivery, transportation providers can optimize resource allocation and enhance the overall performance of their systems. This study introduces a novel methodology that incorporates dwell time uncertainty into paratransit operation systems, specifically focusing on sequentially updating the parameters of the dwell time prediction (DP) model after each request is fulfilled.

This study focuses on the Pickup and Dropoff with Time Windows (PDPTW) problem for paratransit services, a variant of the Vehicle Routing Problem with Time Windows (VRPTW), aiming to identify efficient routes for a fleet of vehicles to serve customers while considering various constraints such as vehicle capacity, time windows, and distance limitations (25, 26). Our focus is primarily on the advanced request scenario, where the problem is defined prior to the need for a solution. In this scenario, customers are required to request services well in advance, allowing for efficient routing of paratransit vehicles before their departure from the depot. Once the vehicles have been dispatched, no additional requests for service can be accommodated.

This study develops a novel approach that involves continuously updating the dwell

time model by sequentially adjusting its parameters. To achieve this, we employ a reinforcement learn- ing (RL) framework (*27–30*). By treating the problem as a sequential decision-making process, the RL framework allows us to learn and adapt the model based on the observed data and feed- back from the environment. This enables us to capture the complex dynamics and dependencies inherent in the PDPTW problem, leading to more accurate and effective predictions of dwell time.

3.2. METHODOLOGY

We now provide a detailed description of the PDPTW problem for paratransit services, present its mathematical formulation, and subsequently introduce the reinforcement learning (RL) framework developed to address this problem.

3.2.1. PROBLEM DESCRIPTION

Figure 1 illustrates the proposed paratransit routing problem, considering customer requests and a dwell time prediction (DP) model. The customer request comprises of pickup and drop-off lo- cations and is implemented as pairwise precedence constraints. These constraints play a crucial role in paratransit operations, ensuring the correct sequence of activities such as picking up customers before dropping them off at their destinations. By incorporating these constraints, valid route construction is simplified.

Each request must be fulfilled within a specified time window and this window is established when a customer requests a pickup and drop-off within a specific time period. The time window specifies the earliest and latest times for service to begin and end. For instance, a para- transit vehicle may be required to pick up a customer from their residence between 8:00 AM and 8:30 AM and drop them off at their destination by 9:00 AM. Time window constraints can make finding feasible routes more challenging but are crucial for ensuring timely service for customers with disabilities or limited mobility.

Each paratransit vehicle has a limited capacity (i.e., whether limited by the total weight of the passengers or the available space, or capacity, of the vehicle, or, in some applications, both weight and capacity limitations) are stationed at a depot and are available to serve the customers during the planning horizon. The planning horizon sets the time frame

within which vehicles must complete their routes, ensuring efficient operation and timely route completion. For example, for 2 a paratransit service that operates from 7:00 AM to 7:00 PM each vehicle would be expected to 3 complete its route within that time frame. Paratransit vehicles are required to return to the depot 4 at the end of the planning horizon. The objective is to optimize the routes taken by the paratransit 5 vehicles to (1) minimize the total travel time of the fleet, (2) fulfill the customer requests on time.

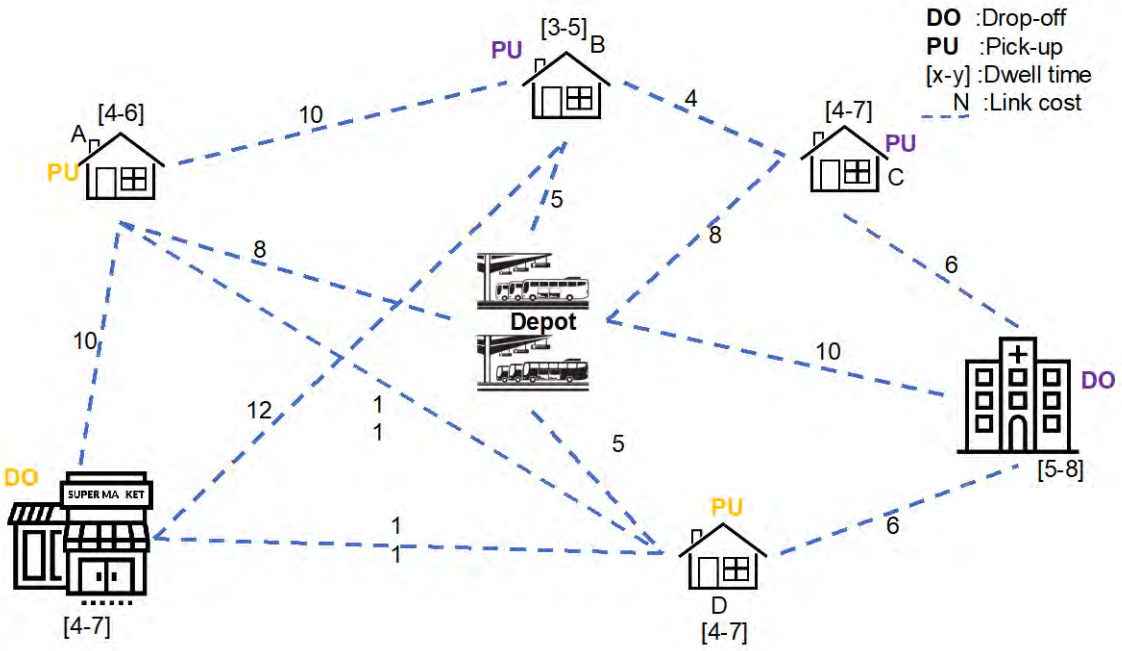

FIGURE 1: Paratransit route optimization to minimize travel time of fleet, fulfill the customer requests on time, and reduce the uncertainty associated with a dwell time prediction Model

To incorporate and update the parameters of the Dwell Time Prediction (DP) model as customer requests are fulfilled, we begin by representing the model's parameters (weights) as a probability distribution with a prior. This prior is learned from historical paratransit service data and captures the initial uncertainty surrounding the parameters. The variance within the prior distribution reflects the level of uncertainty associated with the model. After each request is fulfilled, we use the observed data (actual dwell time) to update the DP model's parameters, resulting in a re-estimation of the probability distribution over the weights, which represents the posterior distribution. Our goal is to use the observed data to maximize the posterior distribution and reduce uncertainty in the model. The

updated posterior distribution provides more accurate knowledge about the model's parameters, allowing us to make more accurate predictions of dwell time and improve overall system performance.

3.2.2. MATHEMATICAL REPRESENTATION

Mathematically, we can express the described problem as follows: The paratransit routing problem is formulated on a graph consisting of three types of vertices: customer pickup vertices denoted as V_{p}, customer drop-off vertices denoted as V_{d}, and depot vertices denoted as V_{dep}. Each vertex i is associated with an array $X_i^t = \left(x_i, z_i, l_i, u_i, \mathrm{dp}_i^t, r_i^t\right)$, where x_i and z_i represents the geographical coordinate of vertex i, l_i (lower bound), and u_i (upper bound), represent the corresponding time 1 window, dp_i^t, is the predicted dwell time (time it takes the bus to complete the request once the bus has arrived at the vertex), and r_i^t is the remaining request at vertex i at step t. The variables dp_i, r_i, and X_i are characterized by the step t because we solve the problem in a sequential manner, and these three elements would change over time. All other elements in X_i^t are static. The time window at the depot is defined as starting from 0 up to the end of the planning horizon denoted as T([0, T]). Additionally, the predicted dwell time and remaining request at this vertex are both set 7 to zero. At each step t, the set of vertex arrays X^t describes the local information at the vertices. The graph is complete, and the weight of each edge (travel time) is the Euclidean distance between the connected vertices. The nodes in the graph have access to a common set of global variables denoted as $G^t = \{\tau^t, \sigma^{2,t}, p^t\}$ where $\tau^t, \sigma^{2,t}$, and p^t indicate the time, variance of the parameter distribution of the DP model, and the number of bus(s) available at the start of step t, respectively. The values of τ^t and p^t are initially set to 0 and the size of the fleet respectively. The initial value of $\sigma^{2,t}$ is the prior variance of the distribution over the weights of the DP model. All the global variables could change over time.

A solution to the paratransit routing problem is represented by a sequence of vertices in the graph, interpreted as the routes taken by buses. The routes for different buses are separated by the depot. For example, if vertex 0 represents the depot, a vertex sequence of {0,2,5,0,4,3,0} corresponds to two routes: one that travels along $0 \rightarrow 2 \rightarrow 5 \rightarrow 0$ and another that travels along $0 \rightarrow 4 \rightarrow 3 \rightarrow 0$. This implies that two buses were used to complete the solution. In order to satisfy the precedence constraint between pick-up and drop-off requests, vertices 2 and 4 are pickup requests, while vertices 5 and 3 are drop-off requests.

3.2.3. REINFORCEMENT LEARNING REPRESENTATION

Looking at the problem of PDPTW for paratransit services from a reinforcement learning perspective, we assume that an agent is responsible for generating a solution to the problem by taking a sequence of actions. At each step, the agent observes the current state of the system and makes an action based on the available information. This action then leads to a change in the system state, and the process repeats until a termination condition is met. To train the agent, we provide it with numerous PDPTW instances and use a reward function to evaluate the solutions it generates. The goal is to guide the agent to improve its performance over time.

The state of the system in this context is described by the information contained in X^t and G^t, which pertain to the graph. An action involves adding a vertex to the end of the current sequence, which is denoted by y^t. The vertex sequence formed up to step t is denoted by Y^t. The termination condition is that all customer requests are satisfied, which occurs at step t_m. At each step t, we estimate the probability of adding each vertex i to the sequence, given G^t, X^t, and travel history Y^t, as $\Pr(y^{t+1} = i \mid X^t, G^t, Y^t)$. We then find the next vertex to visit, y^{t+1}, based on this probability distribution. Finally, we update the system states using transition functions based on y^{t+1} :

$$\tau^{t+1} = \begin{cases} \tau^t + \mathrm{DT}_{y^t} + w(y^t, y^{t+1}), & \text{if } y^t \in V_{\mathrm{p,d}} \\ w(y^t, y^{t+1}), & \text{if } y^t \in V_{\mathrm{dep}} \end{cases}$$

where $w(y^t, y^{t+1})$ is the travel time from vertex y^t to vertex y^{t+1}, DT_{y^t} is the observed (actual) dwell time to pick-up or drop-off customers at vertex y^t (representing the service time at 1 the customer vertex). Next, the variance of the distribution over the weights of the DP model is updated as (31):

$$\sigma^{2,t+1} = \begin{cases} \dfrac{\sigma^{2,t}\sigma^{2,t}}{n\sigma'^{2,t} + \sigma^{2,t}} & \text{if } y^t \in V_{\mathrm{p,d}} \\ \delta'^{2,t}, & \text{otherwise} \end{cases}$$

Where $\sigma^{2,t}$ is the prior variance, $\sigma^{2,t}$ is the new sample variance, and $\sigma^{2,t+1}$ is the posterior variance of the distribution over the weights of the DP model and n is the sample size (new information). Finally, the number of buses available p^t, and the remaining request r_i^t at each vertex are updated as follows:

$$p^{t+1} = \begin{cases} p^t - 1, & \text{if } y^t \in V_{\text{dep}} \\ p^t, & \text{otherwise} \end{cases}$$

$$r_i^{t+1} = \begin{cases} 0, & \text{if } y^t = i \\ r_i^t, & \text{otherwise} \end{cases}$$

We define the reward function for a sequence of vertices, denoted by

$$Y^{t_m} = \{y^0, y^1, \dots, y^{t_m}\},$$

such that a high reward value indicates a high-quality solution. In order to achieve the objective of the problem, which is to minimize the total travel time of the fleet, the variance of the distribution over the weights of the DP model, and the number of vehicles used, we set the first term of equation to be the negative total travel time of the fleet, which prioritizes lower travel time solutions. The second term accounts for the variance of the distribution over the weight of the DP model, making the agent select sequences that minimize the uncertainty of the DP model parameters.

$$r(Y^{t_m}) = \alpha_1 \sum_{t=1}^{t_m} w(y^{t-1}, y^t) + \alpha_2 \sigma^{2,t_m}$$

where $w(y^{t-1}, y^t)$ is the travel time on edge (y^{t-1}, y^t) along trajectory Y^{t_m}, α_1 and α_2 are negative constants.

All additional constraints of the problem, such as the pickup and drop-off precedence constraint, are defined as follows: If the paratransit vehicle is at vertex i at step t and there exists a vertex j (where j is not equal to i) that satisfies any of the specified conditions, we set the transition probability p_i^t to be 0 for moving to that particular vertex.

- Vertex $j \in V_p$ represents unsatisfied pick-up request and the remaining capacity of the bus is zero.
- The earliest arrival time at vertex j violates the time window constraint (i.e., $\tau^t + w(y^{t-1}, y^t) > u_j$)
- Let pre (j) denote the set of nodes that must be visited before node j and Y^{t_i} denote the set of nodes that have already been visited by the agent up to current node i. The node j is

infeasible if $\text{pre}(j) \notin Y^{t_i}$. This masking scheme enforces the pickup and drop-off precedence in the paratransit routing problem. Note that all pickup nodes $(i \notin V_{\text{p}})$ have no precedence nodes (empty set), and each drop-off node $(i \notin V_{\text{d}})$ has exactly one pickup node as precedence.

- We mask all the vertices except the depot if the paratransit vehicle is currently at the depot and there are no remaining customer request vertices.

3.3. NUMERICAL EXAMPLE

In this section, we first provide an exploratory analysis of real-world dwell time distributions, followed by a numerical example using toy data to illustrate and discuss our developed sequential update of the dwell time model. Subsequently, we provide an example that discusses routing scenarios, incorporating relevant route considerations as described in the methodology.

3.3.1. Exploratory analysis of dwell time distribution

Firstly, we performed a cluster analysis on the pick-up longitude and latitude coordinates for sample data from Elizabeth City. Using K-means clustering, we identified eleven distinct clusters. The obtained results in Figure 2a showed a significant clustering performance with an F value of 164.5 and Pr (>F) < 2e-16, indicating statistical significance in the clustering outcome. For each cluster, we constructed its respective dwell time density function (Figure 2b), which characterizes the distribution of dwell times within that specific group.

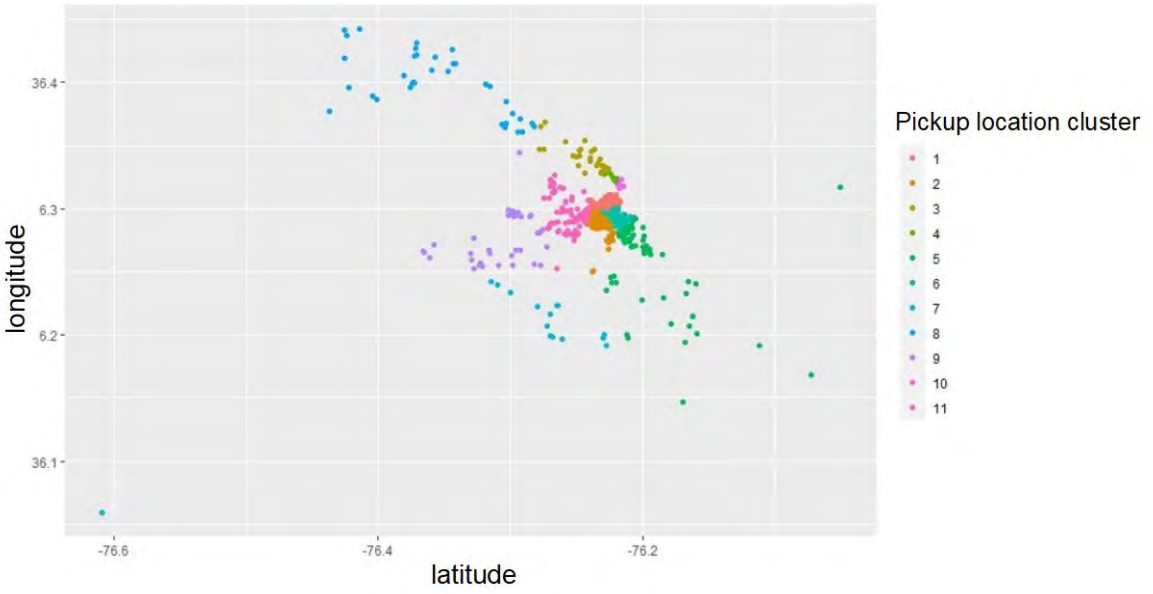

(a) Elizabeth City Scatter plot of pick-up coordinates clusters

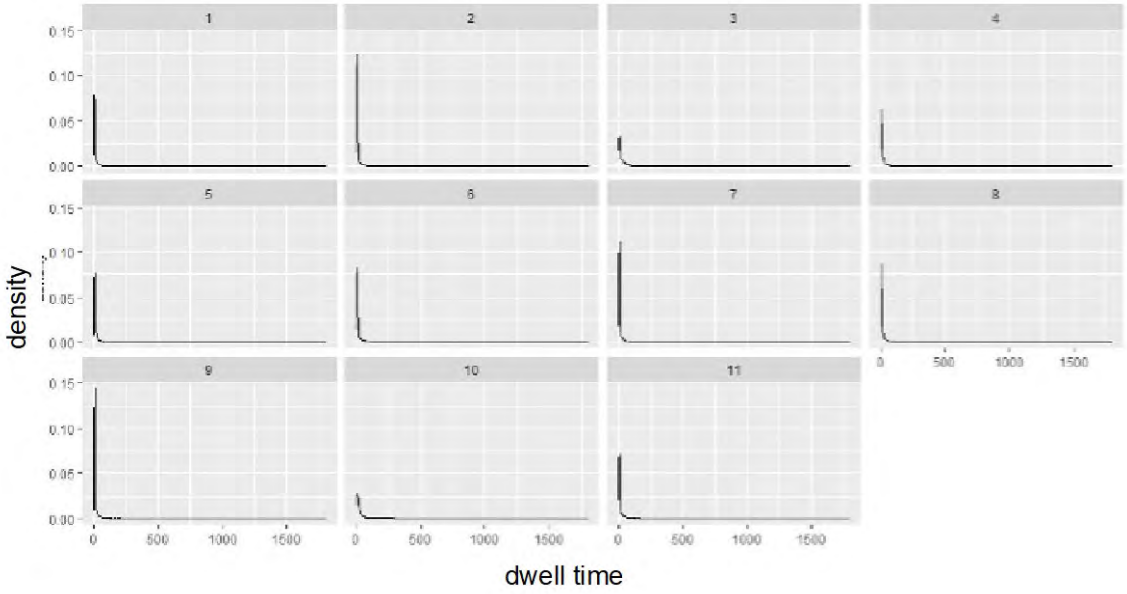

(a) Dwell time density function by cluster

FIGURE 2: Cluster analysis of dwell time data

We observed notable variations in paratransit activity patterns across different geographical regions. Some clusters exhibited higher densities of short dwell times, suggesting efficient drop-off and pick-up processes, while others displayed more extended dwell times, potentially indicating specific locations with higher demand or operational complexities. Figure 3 shows how dwell time varies across different time periods and locations. Longer dwell times may indicate congested or busy stops, while shorter dwell times may reflect efficient boarding and alighting processes. Figure 3a focuses on locations with short dwell times, high- lighting areas where passengers tend to board and alight swiftly. Figure 3b shows medium dwell times, indicating locations where boarding and alighting processes require moderate time. Finally Figure 3c focuses on locations with long dwell times, identifying places or time periods that expe- rience delays during passenger movements. This exploratory analysis yields crucial insights into the dwell time distribution. By observing the spatiotemporal patterns, we can identify potential trends and correlations that can be leveraged in improving predictions of dwell time prediction for future request.

3.3.2. DWELL TIME ESTIMATION MODEL

In exploring the dwell time data, we conducted a logistic regression with a 70% training and 30% testing split, achieving an 89.45% accuracy in distinguishing between the two classes.

The receiver operating characteristic (ROC) curve depicted (Figure 4b) the model's performance by varying the discrimination threshold. An AUC of 0.62 indicated moderate predictive power, correctly classifying 62% of cases, surpassing random guessing (50%), but with room for improvement. The ROC curve's shape aided in selecting an optimal classification threshold.

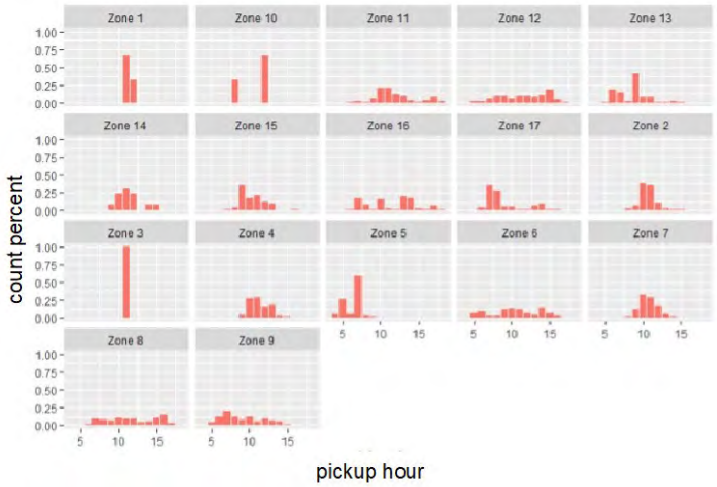

(a) Spatiotemporal distribution of 'short' dwell time

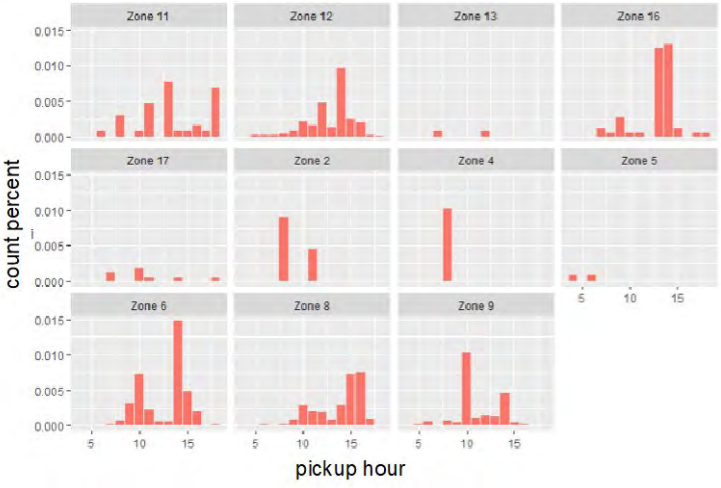

(b) Spatiotemporal distribution of 'moderate' dwell time

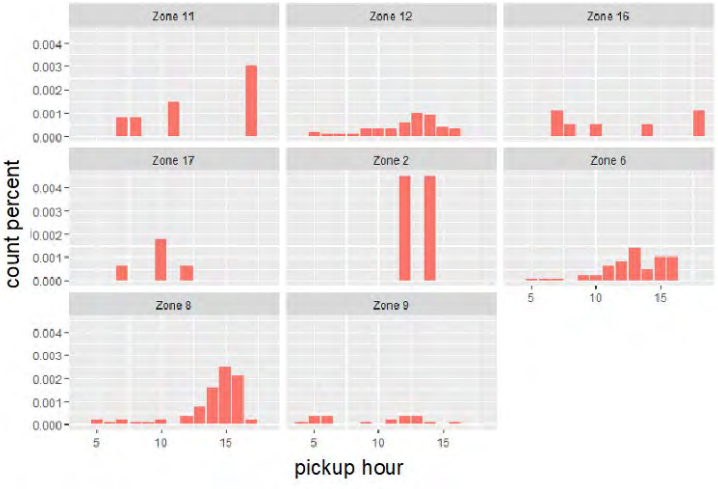

(c) Spatiotemporal distribution of 'long' dwell time

FIGURE 3: Distribution of dwell time classified into three groups

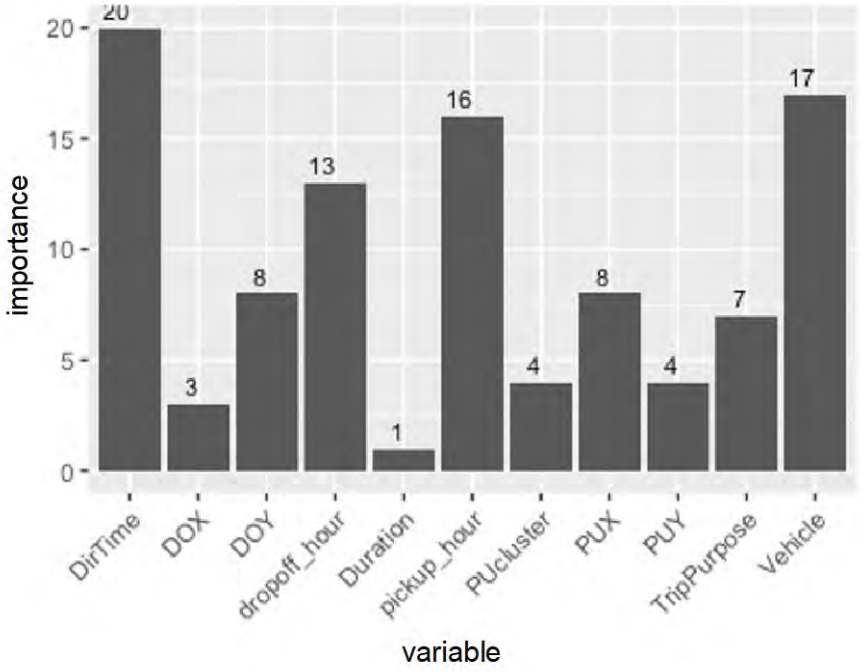

(a) Importance of each variable as a percentage

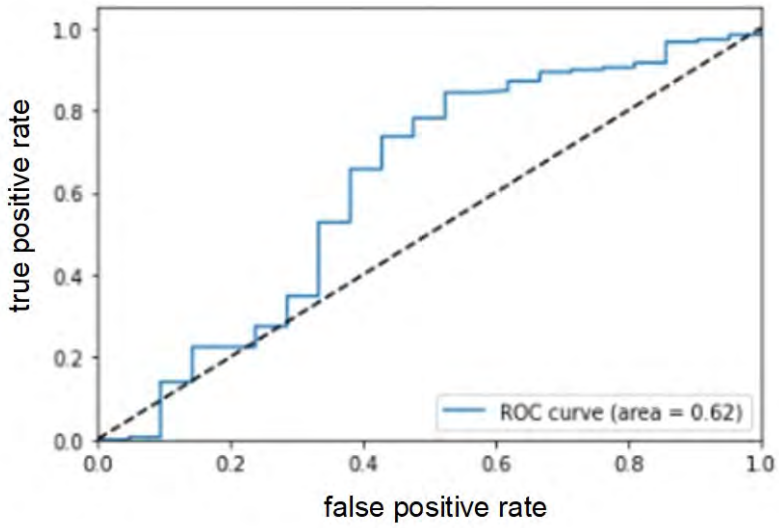

FIGURE 4: Dwell time estimation model analysis

3.3.3. Sequential Updates for the Dwell Time Model

We first illustrate the sequential update process for the dwell time model using Bayesian inference. Specifically, we consider a dwell time model with two weights: Weight 1 and Weight 2. The goal is to iteratively update the mean and variance of these weights based on observed dwell time as each request is served. To demonstrate the sequential update, we perform Bayesian inference for the mean and variance of the weights using the dwell time data in the given scenario. Assuming a normal distribution prior for the weights, we update them sequentially after processing each request.

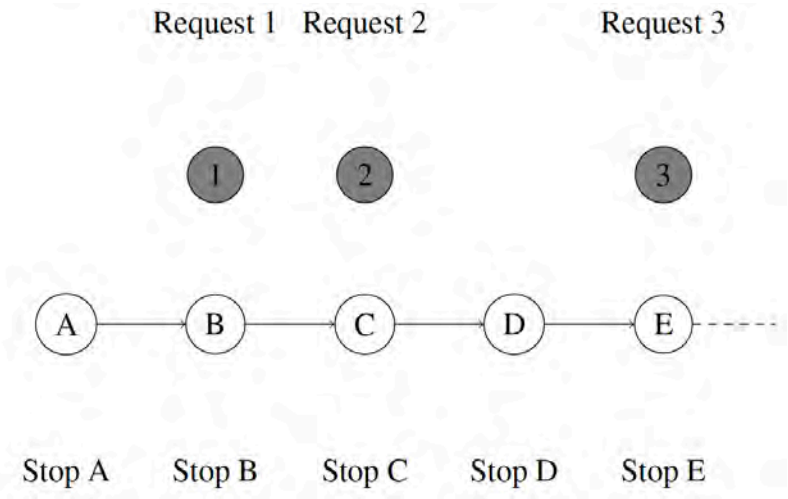

FIGURE 5: Stop sequence and requests

TABLE 1: Assumed values for the computation of updated weights

Description	Assumed Values
Prior Mean (μ_{w1})	3
Prior Variance (σ^2_{w1})	1.5
Prior Mean (μ_{w2})	2
Prior Variance (σ^2_{w2})	2
Likelihood (Request 1)	0.2
Likelihood (Request 2)	0.3

We begin by serving Request 1 at Stop B. The observed dwell time for this request is 4 minutes. We assume a prior distribution for the weights, with a mean (μ) of 3 and a variance (σ 2) of 1.5. Using the current mean and variance values, we compute the likelihood by evaluating the probability density function (PDF) of the normal distribution. In this case, the likelihood (L_1) is calculated as 0.2. Next, we compute the posterior distribution by multiplying the prior distribution with the likelihood. This posterior distribution (P_1) represents the updated belief about the weights given the observed dwell time.

To update the mean and variance of each weight, we use the posterior distribution P_1. The 9 updated mean (μ') and variance $\left(\sigma^{2'}\right)$ are computed using the formulas derived from Bayesian 10 inference. In this case, the updated mean is approximately 3.178 , and the updated variance is 11 approximately 0.171. $\mu = \frac{1.5\times4+3\times0.2}{1.5+0.2} \approx 3.178 \sigma^2 = \frac{1}{\frac{1}{1.5}+\frac{1}{0.2}} \approx 0.171$

Moving on to Request 2 at Stop C, the observed dwell time for this request is 5 minutes. We calculate the likelihood (L_2), resulting in a value of 0.3. Using the updated mean (μ) and variance (σ 2) from the previous step as the prior distribution, we compute the posterior distribution for Request 2. This posterior distribution (P_2) represents the refined belief about the weights after considering the new observation. Similarly, we update the mean and variance of each weight using the posterior distribution P_2. These updated values represent the improved estimates of the weights after incorporating the observed dwell time for Request 2. The sequential update process continues for each subsequent request (Table 2), allowing the dwell time model to adapt and refine its parameters based on the observed data. This iterative Bayesian model update ensures that the dwell time predictions become more accurate and reliable as more requests are served.

TABLE 2: Sequential update process for DT model as requests are served

Request	Stops	Observ. DT	μ_{w1}	σ^2_{w1}	μ_{w2}	σ^2_{w2}	Pred. DT
-	A	-	3	1.5	2	2	[5,6,7]
1	B	4	3.178	0.171	2	2	[6.34,7.17]
2	C	5	3.625	0.2813	2.5	1.5	[8.625]
-	D	-	3.625	0.2813	2.5	1.5	[8.625]
3	E	7	4.1563	0.2109	2.9688	1.1719	[]
-	A	-	4.1563	0.2109	2.9688	1.1719	[]

3.3.4. Optimal customer service sequence

Figure 6 presents a simple numerical example for a typical paratransit service serving customers. The options are organized based on the assignment of customers to two available vehicles, referred to as Vehicle 1 and Vehicle 2. Each routing option is denoted by a distinct combination of customers served by the respective vehicles, and their corresponding total travel times are provided for evaluation. A critical aspect of this paratransit service lies in the constraint of feasible routing options, which is determined by the pickup and drop-off time windows. These time windows play an important role in ensuring that the service adheres strictly to predefined time constraints.

Table 4 provides further details about the characteristics of each customer request. Each row represents a different customer, identified by their unique identifier (Customer a, b, c, d, and e). The table includes information about the pickup location, drop-off location, pickup time window, drop-off time window, mobility need, and time of day for each customer's trip.

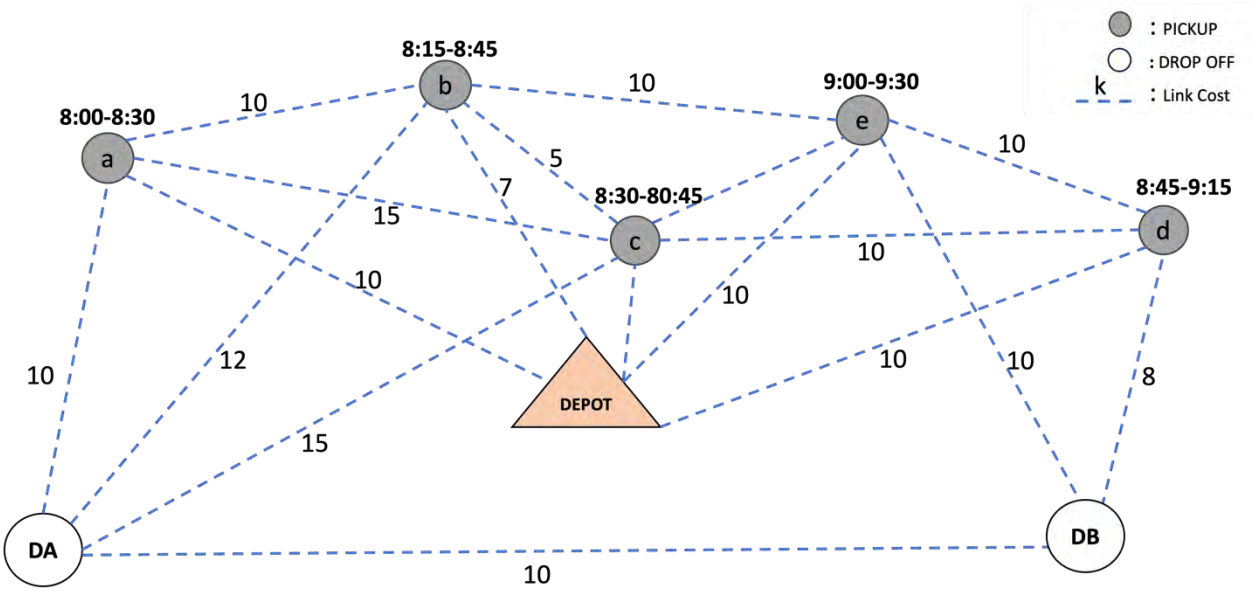

FIGURE 6: Simple numerical example for a typical paratransit service serving customers

Looking at Figure 6, three main options satisfy the PU/DO constraints time window of the customers. In Table 4, we present the various routing options for serving customers in our paratransit service, along with their corresponding total travel times. In option 1, Vehicle 1 serves customers a, b, and c, in that order with a total travel time of 40 minutes, while Vehicle 2 serves customers d and e, with a travel time of 30 minutes, leading to a combined total travel time of 70 minutes. Similarly, option 2 involves Vehicle 1 serving customers b, a, and c, resulting in a travel time of 47 minutes, and Vehicle 2 serving customers d and e, with a travel time of 30 minutes. This results in a combined total travel time of 77 minutes. The best routing option estimated as option. In this configuration, one vehicle serves all the customers efficiently in this order a, b, c, d, and e, leading to a total travel time of 65 minutes. This arrangement achieves a notably reduced total travel time. Compared to the options 1 and 2, option 3 reduces travel time by 7.14% and 15.58% respectively. By choosing the most efficient routing, the service providers can ensure timely and satisfactory transportation for all customers while optimizing resource utilization.

TABLE 3: Customer Requests and Travel Times

R	PU Loc.	DO Loc.	PU TW	DO TW	Mobility Need	Time of Day
a	A1	DA	8:00 AM	9:00 AM	2 (cane)	1 (afternoon)
			−8: 30AM	−9: 30 AM		
b	A2	DA	8: 15AM	9: 15 AM	1 (no support)	1 (afternoon)
			−8: 45AM	−9: 45 AM		
c	A3	DA	8:30 AM	9: 30AM	3 (wheelchair)	1 (afternoon)
			-9:00 AM	−10: 00 AM		$C^2 + s^2$
d	B1	DB	8: 45 AM	9:45 AM	2 (cane)	2 (morning)
			−9: 15 AM	−10: 15 AM	$x^2 + 2 + 3$	
e	B2	DB	9:00 AM	10:00 AM	3 (wheelchair)	2 (morning)
			−9: 30AM	−10: 30AM		-5

TABLE 4: Routing Options and Total Travel Time

Routing Option	Vehicle 1 Customers	Vehicle 2 Customers	Total Travel Time (min)
Option 1	a, b, c	d, e	70
Option 2	b, a, c	d, e	77
Option 3	a, b, c, d, e,	-	65

3.4. CONCLUSION

In this work, we presented a sequential update process for a dwell time model in the context of para- transit routing. The complexity of this problem is further compounded by the dynamic and uncertain nature of dwell time, necessitating the use of efficient and adaptive learning techniques to yield effective solutions for pick-up and delivery problem with uncertain time window. We develop a data-driven reinforcement learning to minimize total delays for a sequence of on-demand requests, while anticipating dwell times based on specific characteristics. By incorporating Bayesian inference, we demonstrated how to refine the model's parameters after each served request, considering both the observed dwell time and the prior information. A novel paratransit routing proactively anticipates the dwell time considering the diverse context of requests in serving individuals with disabilities and the elderly.

Through a numerical example, we illustrated the sequential update process for a dwell time model with two weights. We computed the likelihood of each observation, updated the posterior distribution using the prior and likelihood, and obtained the updated mean and variance of the weights. The sequential update process allows the dwell time model to adapt and improve its pre- dictions over time. By incorporating the observed dwell times, the model becomes more accurate and reliable in estimating future dwell times for unserved requests. The presented work highlights the application of Bayesian inference in paratransit routing, specifically in optimizing travel time and minimizing uncertainty in dwell time predictions. The sequential update process enables the model to learn from the observed data, resulting in improved routing decisions and better overall service quality.

The proposed framework makes a significant contribution to the optimization of paratransit routing by obtaining accurate and reliable estimates for a sequence of requests which can be a significant portion of service time for paratransit. By simultaneously reducing in-vehicle travel time and uncertainty in dwell time predictions, it offers the potential for enhancing the overall quality of paratransit service, resulting in improved transportation experiences for individuals with disabilities and the elderly. Future research can explore

more sophisticated dwell time models and investigate the impact of different prior distributions on the update process. Additionally, incorporating additional factors such as passenger characteristics or traffic conditions can further enhance the accuracy and robustness of the dwell time predictions.

3.5 REFERENCES

1) Dantzig, G. B. and J. H. Ramser, The truck dispatching problem. Management science, Vol. 6, No. 1, 1959, pp. 80–91.

2) Toth, P. and D. Vigo, The vehicle routing problem. SIAM, 2002.

3) Bertsimas, D. J., A vehicle routing problem with stochastic demand. Operations Research, Vol. 40, No. 3, 1992, pp. 574–585.

4) Ehmke, J. F., A. M. Campbell, and B. W. Thomas, Optimizing for total costs in vehi- cle routing in urban areas. Transportation Research Part E: Logistics and Transportation Review, Vol. 116, 2018, pp. 242–265.

5) Wang, Y., X. Ma, Y. Lao, Y. Wang, and H. Mao, Vehicle routing problem: simultaneous deliveries and pickups with split loads and time windows. Transportation research record, Vol. 2378, No. 1, 2013, pp. 120–128.

6) Cattaruzza, D., N. Absi, and D. Feillet, Vehicle routing problems with multiple trips. Annals of Operations Research, Vol. 271, 2018, pp. 127–159.

7) Braekers, K., K. Ramaekers, and I. Van Nieuwenhuyse, The vehicle routing problem: State of the art classification and review. Computers & industrial engineering, Vol. 99, 2016, pp. 300–313.

8) Konstantakopoulos, G. D., S. P. Gayialis, and E. P. Kechagias, Vehicle routing problem and related algorithms for logistics distribution: A literature review and classification. Operational research, 2020, pp. 1–30.

9) Lin, T.-m. and N. H. Wilson, Dwell time relationships for light rail systems. Transportation Research Record, , No. 1361, 1992.

10) Fernandez, R., P. Zegers, G. Weber, A. Figueroa, and N. Tyler, Platform height, door width and fare collection on public transport dwell time: A laboratory study. In 12th

World Conference on Transport Research, 2010, pp. 1–19.

11) Soltani, A., M. Tanko, M. I. Burke, and R. Farid, Travel patterns of urban linear ferry passengers: analysis of smart card fare data for Brisbane, Queensland, Australia. Transportation Research Record, Vol. 2535, No. 1, 2015, pp. 79–87.

12) Mumayiz, S., Evaluating performance and service measures for the airport landside. Trans- portation Research Record, Vol. 1296, 1990, p. 23.

13) Sadeghpour, M. and K. S. Ög˘üt, Analyzing passenger boarding and alighting service times for bus transportation in I˙stanbul, 2017.

14) Gupta, D., H.-W. Chen, L. A. Miller, and F. Surya, Improving the efficiency of demand-responsive paratransit services. Transportation research part A: policy and practice, Vol. 44, No. 4, 2010, pp. 201–217.

15) Cokyasar, T., A. Subramanyam, J. Larson, M. Stinson, and O. Sahin, Time-constrained ca- pacitated vehicle routing problem in urban e-commerce delivery. Transportation Research Record, Vol. 2677, No. 2, 2023, pp. 190–203.

16) Glick, T. B. and M. A. Figliozzi, Analysis and application of log-linear and quantile regression models to predict bus dwell times. Transportation Research Record, Vol. 2673, No. 10, 2019, pp. 118–128.

17) Padmanaban, R., L. Vanajakshi, and S. C. Subramanian, Estimation of bus travel time incorporating dwell time for APTS applications. In 2009 IEEE Intelligent vehicles sympo- sium, IEEE, 2009, pp. 955–959.

18) Csiszár, C. and Z. Sándor, Method for analysis and prediction of dwell times at stops in local bus transportation. Transport, Vol. 32, No. 3, 2017, pp. 302–313.

19) González, E. M., M. G. Romana, and O. M. Álvaro, Bus dwell-time model of main urban route stops: case study in Madrid, Spain. Transportation research record, Vol. 2274, No.

1, 2012, pp. 126–134.

20) Klumpenhouwer, W. and S. Wirasinghe, Optimal time point configuration of a bus route-A Markovian approach. Transportation Research Part B: Methodological, Vol. 117, 2018, pp. 209–227.

21) Garnier, C., M. Trepanier, and C. Morency, Adjusting dwell time for paratransit services.

22) Transportation Research Record, Vol. 2674, No. 9, 2020, pp. 638–648.

23) Wu, F., REAL-TIME SCHEDULING ON A TRANSIT BUS ROUTE. In Computer-Aided Transit Scheduling: Proceedings of the Fifth International Workshop on Computer-Aided Scheduling of Public Transport held in Montréal, Canada, August 19–23, 1990, Springer Science & Business Media, 2012, Vol. 386, p. 213.

24) Li, Y., J.-M. Rousseau, and M. Gendreau, Real-time dispatching of public transit operations with and without bus location information. In Computer-Aided Transit Scheduling: Proceedings of the Sixth International Workshop on Computer-Aided Scheduling of Public Transport, Springer, 1995, pp. 296–308.

25) Li, Y., J.-M. Rousseau, and F. Wu, Real-time scheduling on a transit bus route. In Computer-Aided Transit Scheduling: Proceedings of the Fifth International Workshop on Computer-Aided Scheduling of Public Transport held in Montréal, Canada, August 19–23, 1990, Springer, 1992, pp. 213–235.

26) Savelsbergh, M. W., The vehicle routing problem with time windows: Minimizing route duration. ORSA journal on computing, Vol. 4, No. 2, 1992, pp. 146–154.

27) Desrochers, M., J. Desrosiers, and M. Solomon, A new optimization algorithm for the vehicle routing problem with time windows. Operations research, Vol. 40, No. 2, 1992, pp. 342–354.

28) Lin, B., B. Ghaddar, and J. Nathwani, Deep reinforcement learning for the electric vehi-

cle routing problem with time windows. IEEE Transactions on Intelligent Transportation Systems, Vol. 23, No. 8, 2021, pp. 11528–11538.

29) Rabecq, B. and R. Chevrier, A deep learning Attention model to solve the Vehicle Routing Problem and the Pick-up and Delivery Problem with Time Windows. arXiv preprint arXiv:2212.10399, 2022.

30) Garces, D., S. Bhattacharya, S. Gil, and D. Bertsekas, Multiagent Reinforcement Learning for Autonomous Routing and Pickup Problem with Adaptation to Variable Demand. arXiv preprint arXiv:2211.14983, 2022.

31) Peng, B., J. Wang, and Z. Zhang, A deep reinforcement learning algorithm using dynamic attention model for vehicle routing problems. In Artificial Intelligence Algorithms and Applications: 11th International Symposium, ISICA 2019, Guangzhou, China, November 16–17, 2019, Revised Selected Papers 11, Springer, 2020, pp. 636–650.

32) Murphy, K. P., Conjugate Bayesian analysis of the Gaussian distribution. def, Vol. 1, No. 2σ 2, 2007, p. 16.